Published in final edited form as:
Physiol Genomics. 2008 June 12; 34(1): 112–126. doi:10.1152/physiolgenomics.00239.2007.

The in vivo Gene Expression Signature of Oxidative Stress

Eun-Soo Han[*,1], **Florian L. Muller**[*,2], **Viviana Perez**[*,2], **Wenbo Qi**[2], **Huiyun Liang**[2], **Liang Xi**[1], **Chunxiao Fu**[1], **Erin Doyle**[1], **Morgen Hickey**[1], **John Cornell**[3,5], **Charles J. Epstein**[6], **L. Jackson Roberts**[7], **Holly Van Remmen**[2,4,5], and **Arlan Richardson**[2,4,5]

1*Department of Biological Science, University of Tulsa, 600 S. College Ave. Tulsa, Oklahoma 74104, USA*

2*Department of Cellular and Structural Biology, University of Texas Health Science Center at San Antonio, San Antonio, Texas 78229-3900*

3*Department of Barshop Institute for Longevity and Aging Studies, University of Texas Health Science Center at San Antonio, San Antonio, Texas 78229-3900*

5*Center for Epidemiology and Biostatistics, University of Texas Health Science Center at San Antonio*

4*GRECC, South Texas Veterans Health Care System, San Antonio, Texas 78284-7762*

6*Department of Pediatrics, University of California, San Francisco, 94143*

7*Departments of Pharmacology and Medicine, Vanderbilt University, Nashville, Tennessee 37232*

Abstract

How higher organisms respond to elevated oxidative stress *in vivo* is poorly understood. Therefore, we measured oxidative stress parameters and gene expression alterations (Affymetrix arrays) in the liver caused by elevated reactive oxygen species induced *in vivo* by diquat or by genetic ablation of the major antioxidant enzymes, CuZn-Superoxide Dismutase (*Sod1*) and Glutathione Peroxidase-1 (*Gpx1)*.

Diquat (50 mg/kg) treatment resulted in a significant increase in oxidative damage within 3 to 6 hours in wild type mice without any lethality. In contrast, treating *Sod1*$^{-/-}$ or *Gpx1*$^{-/-}$ mice with a similar concentration of diquat resulted in a significant increase in oxidative damage within an hour of treatment and was lethal, i.e., these mice are extremely sensitive to the oxidative stress generated by diquat. The expression response to elevated oxidative stress *in vivo* does not involve an upregulation of classical antioxidant genes, though long-term oxidative stress in the *Sod1*$^{-/-}$ mice leads to a significant upregulation of thiol antioxidants (e.g., *Mt1*, *Srxn1*, *Gclc*, *Txnrd1*), which appears to be mediated by the redox-sensitive transcription factor, *Nrf2*. The main finding of our study is that the common response to elevated oxidative stress, with diquat treatment in wild type, *Gpx1*$^{-/-}$, *Sod1*$^{-/-}$ mice and in untreated *Sod1*$^{-/-}$ mice, is an upregulation of p53 target genes (*p21*, *Gdf15*,

Address correspondence to: Arlan Richardson, Barshop Institute for Longevity and Aging Studies, University of Texas Health Science Center at San Antonio, Texas Research Park Campus, 15355 Lambda Drive, San Antonio, TX 78245-3207; Phone: 210-562-6140; Fax. 210-562-6110; E-mail: RICHARDSONA@uthscsa.edu.

*These authors contributed equally to this work

*The authors would like to acknowledge the assistance of Marian Sabia, Jay Cox, Vivian Diaz and Amanda Jernigan for excellent mouse husbandry. Financial support was provided by NIA training grant #5T3-AG021890-02 (FLM), NIH grant AG-14674-04S1 and EPSCoR-2004-99 from Oklahoma State Regents for Higher Education (ESH), NIH grants P01 AG19316, P01AG020591, R01 AG 23843, R37 AG026557 (AR), NIH R37 GM42056 (LJR), and the San Antonio Nathan Shock Aging Center (1P30-AG13319), and VA Merit grants (AR & HVR) and a REAP from the Department of Veteran Affairs. We would also like to express our thanks to Alex Bokov for assistance with Microsoft Excel and Drs. William Boylston and Yousin Suh for stimulating conversations.

[2]For an extensive comparison of microarray vs. "true" fold changes see Table 2 and 3 [in reference (1)].

[3]Sulfiredoxin, also known as *Npn3* or Neoplastic progression 3, is the most strongly inducible, *Nrf2*- dependent gene [see reference (48)].

Plk3, *Atf3*, *Trp53inp1*, *Ddit4*, *Gadd45a*, *Btg2*, *Ndrg1*). A retrospective comparison with previous studies shows that induction of these p53-target genes is a conserved expression response to oxidative stress, *in vivo* and *in vitro*, in different species and different cells/organs.

Keywords

Oxidative Stress; Gene Expression; p53-target genes; Sod1; Gpx1

INTRODUCTION

Reactive oxygen species (ROS[1]) such as superoxide ($O_2^{\cdot -}$/$HO_2^{\cdot -}$), hydrogen peroxide (H_2O_2) and the hydroxyl radical ($OH^{\cdot}$) are deleterious by-products of aerobic metabolism (14,61). ROS can be pathogenic (6,62,82), and if left unchecked, are incompatible with life in higher organisms (20,22,49,54,63). Oxidative damage to cellular components by ROS can compromise the structure and function of a variety of macromolecules, e.g., DNA, lipids, and proteins (6,77). This in turn can lead to impaired physiological function and has been suggested as a cause of a variety of diseases and aging (6,32,82).

An elaborate network, which is not completely understood, of non-enzymatic and enzymatic antioxidant defense mechanisms has evolved to cope with ROS. The best characterized non-enzymatic ROS scavengers include the antioxidant vitamins E and C, as well as glutathione and thioredoxin. However, this picture is likely far from complete, e.g., the biliverdin/bilirubin system has recently been discovered to function as an antioxidant (4). The main enzymatic branches of the antioxidant network include the superoxide dismutases (SOD), the glutathione peroxidases (GPX), the peroxiredoxins and catalase (28,88). The SODs catalyze the dismutation of superoxide into oxygen and hydrogen peroxide (58). The latter is then converted to water by either catalase, the glutathione peroxidases or peroxiredoxin families [which of these is most relevant and under what circumstances is not yet fully understood (88)]. There are three mammalian superoxide dismutases: cytosolic CuZnSOD (*Sod1*) the most abundant (58), mitochondrial matrix MnSOD (*Sod2*) (85), and extracellular SOD (EC-SOD, *Sod3*) (57). There are at least four glutathione peroxidases (*Gpx1* through *4*) and six peroxiredoxins (*Prdx1* through *6*) in mammalian cells. The cytosolic/mitochondrial selenoprotein Gpx1 is traditionally thought to be the main scavenger of cellular H_2O_2 (28) but the importance of peroxiredoxins is increasingly recognized (50,63,83).

The inner workings and interrelationships within the antioxidant system *in vivo* are at present poorly understood. While it is clear that ROS can play a role in modulating cell signaling [reviewed in (24)], how the antioxidant system and indeed the cell as a whole responds to elevated oxidative stress *in vivo* is not well understood. Studies in this area have largely been conducted with cells in culture (18,19). With regard to oxidative stress, this presents a strongly confounding factor because culturing cells under atmospheric oxygen tension (21% versus physiological oxygen tension of ~5%) is now well established to be a potent oxidative stress in itself (13,38,67). Indeed, even though *Sod1*$^{-/-}$ mice are viable, cells from *Sod1*$^{-/-}$ mice do not grow under standard culture conditions (11,41). Another potential problem with cell culture is whether the type and degree of oxidative stress applied is physiologically relevant (for example, is the application of a bolus dose of 100 μM H_2O_2 representative of a possible *in vivo* situation).

[1]The abbreviations used are: ROS: Reactive oxygen species; Sod: Superoxide dismutase; Gpx: glutathione peroxidase; WT: wild type; ALT: Alanine Amino transferase; DQ: Diquat; 8-oxo-dG: 8-oxo-2-deoxyguanosine.

In this study, we measured global changes in gene expression induced by oxidative stress *in vivo* in liver using Affymetrix arrays. We employed a dual strategy to induce oxidative stress (which we quantified by measuring oxidative damage to DNA and lipids), namely the injection of mice with the redox-cycler diquat (78) and/or the ablation of the major antioxidant enzymes Sod1 and Gpx1 (34,41). Oxidative stress is thus induced via unchecked production of ROS from endogenous physiological sources as well as the overproduction of ROS by the exogenously added diquat. We observed no increased upregulation of classical antioxidant enzymes in the livers of either WT, *Gpx1*$^{-/-}$ or *Sod1*$^{-/-}$ mice treated with diquat even though diquat induced a dramatic increase in oxidative stress *in vivo* in the livers of these mice. However, untreated *Sod1*$^{-/-}$ mice, which exhibited a significant increased oxidative stress compared to untreated WT and *Gpx1*$^{-/-}$ mice, showed a significant increase in thiol-based antioxidant defense genes.

We identified a panel of genes that showed a common pattern of gene expression in response to both endogenous and exogenous oxidative stress *in vivo*: an upregulation of *p53*-target, checkpoint genes. To our knowledge this is the first study to identify *p53*-target genes as a common response of cells/tissues to oxidative stress.

EXPERIMENTAL PROCEDURES

Animals

C57BL/6J mice used in this study were obtained from the aging colonies of mice maintained by the San Antonio Nathan Shock Aging Center (originally purchased from The Jackson Laboratory, Bar Harbor, ME). *Sod1*$^{-/-}$ and *Gpx1*$^{-/-}$ mice were generated in the laboratories of C. Epstein and Y.S. Ho, respectively (34,41). These mice were maintained in the heterozygous state on a C57BL/6J background (backcrossed for over 10 generations) under specific pathogen free conditions. All the mice were male, 3-6 months of age, group housed, at 4 animals per cage, and fed *ad libitum* Harlan Teklad LM-485 mouse/rat sterilizable diet 7912 (Madison, WI). Mice were maintained on a 12:12 h light-dark cycle (lights on at 6:00 A.M.). Diquat was delivered intraperitoneally at 50 mg/kg body mass, a dose chosen because it is not lethal to wild type mice. All animals were sacrificed between 9 and 11 A.M. to minimize potential variation due to circadian rhythms. The rodents were humanely euthanized at 0, 1, 3, 6 and 12 hours (h) after diquat treatment and tissues were immediately collected, frozen in liquid nitrogen, stored at −80°C and analyzed within 30 days. All procedures for handling the mice were approved by the Institutional Animal Care and Use Committee of the University of Texas Health Science Center at San Antonio and the Subcommittee for Animal Studies at the Audie L. Murphy Memorial Veterans Hospital.

Oxidative damage and liver necrosis

Plasma alanine aminotransferase (ALT) activity—Plasma ALT activity was measured using a commercially available kit (Transaminases [ALT/GPT and AST/GOT], Sigma) according to the manufacturer's instructions. The ALT activity was calculated from the calibration curve and expressed as Sigma-Frankel (SF) Units/mL (69).

Lipid peroxidation—Lipid peroxidation was measured in mouse plasma and liver by the levels of F_2-isoprostanes. Mouse blood was collected under deep anesthesia, and plasma was isolated by centrifugation. Because of the small volume, it was necessary to pool sera from 3 mice. Mouse livers (~200 mg) were homogenized, and whole lipid extracted with chloroform/heptane. The levels of F2-isoprostanes from blood (free) and liver (esterified) were determined using gas chromatography/mass spectrometry (GC/MS) as initially described by Morrow and Roberts (59) and currently used in this laboratory (84).

DNA oxidative damage—Oxidative damage to nuclear DNA was determined by measuring the levels of 8-oxo-2-deoxyguanosine (8-oxo-dG). Mouse livers were homogenized in Dounce homogenizers in ice-cold lysis solution provided with a DNA Extractor WB kit (Wako Chemicals, Richmond, VA, USA), and nDNA was isolated following instructions of the DNA Extractor WB, and the nuclear DNA was hydrolyzed as described by Hamilton *et al.* (29). The 8-oxo-dG and 2-deoxyguanosine in the hydrolysates were resolved by high-pressure liquid chromatography and quantified by electrochemical detection. The data were expressed as the ratio of nmol of 8-oxo-dG to 10^5 nmol of 2-deoxyguanosine.

Statistical analysis of oxidative damage data—Both the T-test and ANOVA Tukey-Cramer methods were used to analyze the statistical significance of the results. Unless indicated, the P value represents the statistical result from Tukey-Cramer method. $P<0.05$ is considered as statistically significant.

Gene Expression

RNA isolation—Total RNA was extracted from liver tissues of control and diquat-treated wild type, *Sod1*$^{-/-}$, and *Gpx1*$^{-/-}$ mice (RNA was obtained for 7 mice for each group) as previously described (72). The RNA yield of each sample was determined spectrophotometrically, assuming that 1 optical density at 260 nm (OD_{260}) unit = 40 mg/L. The quality of total RNA extracted from each sample was monitored by A260:A280 ratio and 1.0% agarose formaldehyde gel electrophoresis. All samples had 260:280 ratios of ~2 and exhibited discrete 28S and 18S rRNA bands. Several samples were randomly chosen and subjected to Northern Blot analysis for further mRNA quality control using glyceraldehyde-3-phosphate dehydrogenase as a probe to ensure the quality of the RNA samples.

Measurements of mRNA transcripts by Affymetrix GeneChip® arrays—Mouse Expression Array 430 A (MOE430A) GeneChips® were purchased from Affymetrix (Santa Clara, CA). The MOE430A GeneChip® contains approximately 22,000 genes; approximately 14,500 of which are well annotated genes with known full length sequences and the remainder being unknown genes. For the 9 treatment groups, 63 GeneChip® arrays were hybridized (one GeneChip®/mouse, 7 mice/treatment group). Prior to the labeling reaction, RNA samples were subjected to a cleanup process using columns from RNeasy Total RNA Isolation Kit (Qiagen, Valencia, CA). We followed the vendor's protocols for GeneChip® hybridization and scanning (31).

Statistical analysis of microarray data—Affymetrix GeneChip® Operating Software (GCOS version 1.1.1, Affymetrix, Santa Clara, CA) was used to quantify each GeneChip®. The summary intensities for each probe (as contained in the CEL files) were loaded into DNA-Chip Analyzer (dChip) (53), version 1.3 for normalization and standardization. To normalization the arrays, i.e., placing the arrays on a common measurement scale by adjusting for differing “brightness” among arrays that might arise due to amount of starting RNA or labeling efficiency, we used a nonlinear approach that is the method of normalization implemented in the dChip software package. The same software was used to combine probe level data, comprising 11 pairs of 25-mer probes for each gene, into a single gene-specific summary estimate of expression. Upon visual inspection, no array had any obvious contamination or noticeable difference in overall brightness. Array outliers occur when the fitted expression for the entire probe set has an unusually high standard error (≥3 standard deviations away from its corresponding mean) when compared to the other chips. Chips with more than 5% of probe sets flagged as array outliers are of suspect quality; however, dChip did not flag any of the arrays as an outlier. Single outliers are solitary probes of unusual intensity within a chip. In this set of samples, outlier percentages ranged from 0.02% to 0.36%. Single

outliers were treated as missing values in subsequent analyses. The percentage of genes called "present" by the GCOS software ranged from 53.42% to 64.69%.

In order to determine which genes showed a statistically significant change in expression between the comparison groups, we ran unpaired t-tests, a commonly used method to evaluate the differences in means between two groups. The t-test comparison assumes the data are approximately normally distributed, and the variances of the separate groups are approximately equal. For this reason, we standardized and log transformed the data prior to analysis. In order to correct for multiple testing, we calculated the Hochberg and Benjamini (35) false discovery rate (FDR) and set the FDR adjusted p-value (α) for the unpaired t-test results at less than 0.005. The results were further restricted by deleting those probe sets with "absent" GCOS detection calls across all chips in both comparison groups. Considering the Gene Bank Accession number to represent unique genes, we deleted repeated accession numbers except in cases when the probe set name designation indicated that the probe sets recognized alternative transcripts from the same gene. Otherwise, we discarded the repeated accession number results for those probe sets that were not unique to a single gene (see Appendix B in AffyMetrix's Data Analysis Fundamentals manual).

We used Expression Analysis Systematic Explorer (EASE) to statistically test for significant over representation of the Gene Ontology (GO) Consortium category, Biological Process, in our results. Instead of ranking functional clusters by the number of selected genes per category, this software ranked functional clusters by statistical over representation of individual genes in specific categories relative to all genes in the same category. The EASE score is a modification of Fisher's exact test that attenuates the significance of categories carried by a few genes and slightly penalizes categories supported by many genes in order to yield more robust findings.

Real time quantitative reverse transcription polymerase chain reaction (QRT-PCR) assay—QRT-PCR was used to independently verify the changes in mRNA levels identified by Affymetrix arrays. The same sources of RNA used for the GeneChip® array experiments were used for the real time QRT-PCR. Primers were designed using the OligoPerfect™ Designer (Invitrogen, Carlsbad, CA) and purchased from Invitrogen. The data in Webtable III give the primer sequences used and their annealing temperatures. The 18S rRNA was used as an internal control for PCR quantification. PCR reactions were carried out as previously described (25). Relative quantification of gene expression was performed as described previously (16, 25). Briefly, logarithmic transformations of raw fluorescence data from the log-linear portion of real time PCR growth curves for both target and reference genes (18S rRNA in our experiment) were analyzed using a SAS/STAT Mixed Procedure program, which is specifically designed to give a point estimate of the relative expression ratio of the target gene with associated 95% confidence interval.

Tissue fractionations—Liver tissues were homogenized in 50 mM Tris pH 7.4 supplemented with protease inhibitor cocktail (Calbiochem, La Jolla, CA). The homogenates were centrifuged at 600 x *g* for 10 minutes at 4°C; the pellet was used for nuclei isolation and the supernatant was then centrifuged at 10,000 x *g* for 10 minutes at 4°C to obtain the mitochondrial pellet. The supernatant was further centrifuged at 100,000 x *g* for 60 minutes at 4°C yielding the cytosolic fraction.

Nuclei Isolation—Nuclei were obtained by ultracentrifugation of the crude pellet obtained after the first slow centrifugation (600 g for 10 minutes) through 2.2 M sucrose containing 1 mM $MgCl_2$. The nuclei were further purified by two washing at 10,000 g for 10 minutes using a buffer containing 0.32 M sucrose, 1 mM $MgCl_2$, 2 mM $CaCl_2$, 10 mM tris buffer pH. 7.4 and 0.5% Triton X-100. The pellets were resuspended in 10 mM Tris buffer pH.8.0 containing

0.14M NaCl, 1mM $MgCl_2$ and centrifuged at 10,000g for 10 minutes. The final pellet was homogenized in 0.1M Tris buffer pH 7.5 containing 2 mM $MgCI_2$, 2 mM $CaCI_2$ supplemented with protease inhibitor mixture and sonicated (2X 10 seconds). The samples were centrifuged at 10,000 xg for 15 minutes and the supernatant was used for Western blot analysis (8,15).

Mitochondrial extract—The mitochondrial pellet was washed twice with 50 mM Tris buffer pH 7.4 and resuspended in 50 mM Tris buffer pH 7.4 containing 0.5% Triton X-100 and protease inhibitor cocktail. The samples were incubated for 45 minutes at 4°C and centrifuged at 100,000 g for 15 minutes, the pellet was discarded and the supernatants (mitochondrial extracts) were used for Western blot analysis. The protein concentration was determined using the Bradford protein assay reagent (Biorad, Richmond, CA).

Western blot analysis

Samples were lysed in Laemmli buffer containing 100 mM β-mercaptoethanol and 0.4% SDS for 10 minutes at 95°C. The amount of sample loaded varied for each antibody and is indicated in the results. Samples were resolved by SDS/PAGE and transferred onto PVDF membranes. The antibodies used were: rabbit polyclonal antibody anti-Nrf2 (sc-722,), goat polyclonal antibody anti-peroxiredoxin 1 (sc-7381), rabbit polyclonal antibody anti-sulfiredoxin (sc-51211) from Santa Cruz (Santa Cruz, CA). Monoclonal anti-mouse anti-p53 antibody (#2524) and polyclonal anti rabbit phospho-p53 (#9284) were from Cell Signaling Technology (Danvers, MA). Mouse monoclonal anti-Hemeoxygenase-1 (clone # HO-1-1) and mouse monoclonal anti-Metallothionein (clone # UC1MT) antibodies were from Stressgene Bioreagents (Ann Arbor, MI). Rabbit polyclonal anti-Txn-1 (LF-PA002) and mouse monoclonal anti-Txn-2 (MA-0079) antibodies were from Labfrontier, (Seoul, Korea). Mouse monoclonal anti-CD36 (MAB1258) antibody was from Chemicon International, Inc (Temecula, CA) and rabbit polyclonal antibody anti-Gpx4 was generated as described by (91) using a 17-amino-acid peptide corresponding to the C terminal of Gpx4 protein as antigen. The β actin, ATPase β subunit, and histone H1 were used as the loading controls for cytosolic, mitochondrial and nuclear fractions, respectively.

Thioredoxin reductase activity

Thioredoxin reductase activity was measured in the cytosolic fraction, using the 5,5'-dithiobis (2-nitrobenzoic acid)-reduction aurothioglucose inhibition method (27). Briefly, reduction of 5,5'-dithiobis(2-nitrobenzoic acid) by NADPH was followed at absorbance 412 nm. A second assay was performed as described above, with the addition of 20 μM aurothioglucose, a specific inhibitor of thioredoxin reductase. Thioredoxin reductase activity was calculated as the differences between the activities measured in the absence and presence of aurothioglucose, and expressed as relative units per mg of protein extract. The assay was performed on the same cytosolic fractions used for Western blot.

RESULTS

Diquat treatment causes oxidative stress and hepatotoxicity, which is enhanced in mice lacking Sod1 or Gpx1

Before screening the genome for changes in gene expression after an oxidative stress, we first measured the levels of oxidative stress *in vivo* in liver tissue from *Gpx1*$^{-/-}$ and *Sod1*$^{-/-}$ mice before and after injection of diquat, which generates superoxide anions in the liver *in vivo* (45,68,78). Hepatotoxicity induced by diquat can be followed by the extent of liver necrosis, which can be quantified by measuring the levels of ALT in plasma (69). As can be seen in Figure 1A, intraperitoneal injection of 50 mg/kg diquat induced significant liver injury 3-6 h after diquat treatment in wild type mice; there was no significant increase in ALT 1 h after diquat treatment. Because diquat undergoes redox cycling (78) leading to the generation of

superoxide (which will dismutate to H_2O_2), it stands to reason that animals with a deficiency in an antioxidant enzyme would suffer more severe toxicity when exposed to diquat. While all wild type (WT), control mice survived 50 mg/kg diquat (data not shown), the two knockout models were unable to survive more than a few hours after this dose of diquat. *Sod1*$^{-/-}$ mice died 1-3 h (mean±S.E.M.: 1.45±0.26 h, N=4) after diquat administration, and the *Gpx1*$^{-/-}$ mice died after 4-6 h (mean±S.E.M.: 3.84±0.30 h, N=6). The data in Figure 1B show that *Gpx1*$^{-/-}$ and *Sod1*$^{-/-}$ mice showed increased hepatotoxicity to diquat in 1 h after treatment as measured by ALT levels. When *Gpx1*$^{-/-}$ mice were treated with diquat, they showed a 120% increase in plasma ALT activity 1 h after diquat injection that was statistically significant compared to the diquat-treated WT and untreated *Gpx1*$^{-/-}$ mice. *Sod1*$^{-/-}$ mice showed an even greater increase (200%) in ALT activity, which was significantly greater than either the diquat-treated WT or untreated *Sod1*$^{-/-}$ mice. There were no differences in ALT levels between untreated knockout and WT mice.

Diquat is a superoxide generator, and it is recognized that the hepatotoxicity resulting from diquat treatment arises from oxidative stress/damage (33,70,76). We quantified the level of oxidative stress after diquat administration by measuring oxidative damage to lipids and DNA. Lipid peroxidation was assessed by measuring the levels of F_2-isoprostanes, which are stable, prostaglandin-like products formed *in vivo* by free radical-catalyzed non-enzymatic, cyclooxygenase-independent peroxidation of arachidonic acid (60). These are formed during lipid peroxidation reactions in lipid membrane bilayers and are subsequently cleaved and eliminated via plasma (59). As shown in Figure 2A and B, both plasma free F_2-isoprostanes (that is, those that have been cleaved from lipids and are in the free-fatty acid form in the process of being eliminated) and liver total lipid esterified F_2-isoprostanes (that is F_2-isoprostanes still in the complex lipids in membranes) were significantly increased 3-6 h after diquat treatment in WT mice. Plasma free F_2-isoprostanes, but not esterified liver F_2-isoprostanes, significantly increased as early as 1 h after diquat injection in WT mice. Compared to the WT mice, *Gpx1*$^{-/-}$ mice had significantly higher levels of plasma free F_2-isoprostanes and liver total F_2-isoprostanes 1 h after diquat treatment. Again, diquat-treated *Sod1*$^{-/-}$ mice showed even higher plasma free and liver esterfied F_2-isoprostanes levels compared to diquat-treated *Gpx1*$^{-/-}$ mice and WT mice (Figure 2C and D). Importantly, untreated *Sod1*$^{-/-}$ mice had significantly higher basal plasma free F_2-isoprostane levels than *Gpx1*$^{-/-}$ mice, which had the same basal F_2-isoprostane levels as WT mice (Figure 2B). It is worth noting that plasma F_2-isoprostanes exhibited a much greater increase after diquat than did liver esterfied F_2-isoprostanes. This effect has been described previously (3), and a similar phenomenon is seen in the untreated *Sod1*$^{-/-}$ mice (Figure 2).

Oxidative stress was also measured in liver by the presence of 8-oxo-dG in nDNA, which is one of the most widely used markers for DNA oxidative damage (30). In wild type mice, 8-oxo-dG levels in liver increased after diquat treatment, and reached statistical significance at 3-6 h. Mice lacking Gpx1 had significantly higher 8-oxo-dG levels than WT mice 1 h after diquat treatment, while *Sod1*$^{-/-}$ mice showed even higher 8-oxo-dG levels than *Gpx1*$^{-/-}$ mice 1 h after diquat treatment. Like the basal plasma free F_2-isoprostanes level, the basal level of 8-oxo-dG in *Sod1*$^{-/-}$ but not *Gpx1*$^{-/-}$ mice was again higher than that of WT (Figure 3B).

Diquat treatment causes dramatic changes in global gene expression

Because diquat induces oxidative stress, which peaked at 3 to 6 h after injection, gene expression was measured in the liver tissues of male C57BL/6 WT mice at 0 (control, no diquat treatment), 1, 3, 6, and 12 h after diquat injection. Comparisons of the control (untreated) WT mice with each of the four groups treated with diquat (1h DQ, 3h DQ, 6h DQ, and 12h DQ) were carried out to identify genes whose expression are altered by diquat. The number of genes whose expression changed significantly ($p<0.005$) by diquat treatment at the various time

points (as compared to the untreated control) are presented in Webtable V (see Webtable I at http://www.jbc.org for gene names, gene bank accession numbers, fold changes, and p-values). Webtable V shows that the expression of 245, 1237, 1642, 4129 genes was altered at 1 h, 3 h, 6 h, and 12 h following diquat, respectively. EASE analysis of gene ontologies "Biological Process" is presented in Webtable II Also indicated in Webtable V (Row five) are the number of genes altered at any given time point of diquat treatment (4551 unique genes), as well as those genes found to show significantly different levels of expression at all time periods after diquat injection compared to untreated control samples (153 genes; 60 increased, 93 decreased). To judge the relative magnitude of the gene expression changes, these are further subdivided into the number of genes whose expression was significantly changed more than 1.5-, 2-, and 2.5-fold. The number and magnitude of gene expression alterations increased throughout the time course of diquat treatment as shown in Table I.

Global changes in gene expression are more extensive in the Sod1$^{-/-}$ than in the Gpx1$^{-/-}$ mice

We next investigated the effect of ablating the two major antioxidant enzymes, Sod1 and Gpx1 on gene expression in the liver. In these experiments, *Sod1*$^{-/-}$ and *Gpx1*$^{-/-}$ mice were either untreated or treated with diquat for 1 h, and gene expression was compared to wild type mice either untreated or treated with diquat for an hour. The data in Webtable VI show that 1404 (638 up and 766 down regulated) genes were changed in the untreated *Sod1*$^{-/-}$ mice (Row 3) and 648 (245 increased, 403 decreased) genes were changed in the untreated *Gpx1*$^{-/-}$ mice (Row 1) with respect to untreated WT mice. As Webtable VI shows, when considering the larger fold changes (>2 fold and >2.5 fold), the number of genes altered in the untreated *Sod1*$^{-/-}$ is greater than in the untreated *Gpx1*$^{-/-}$ mice (43 vs. 14 genes altered more than 2.5-fold). Thus, the gene expression changes in the untreated *Sod1*$^{-/-}$ are both greater in number and magnitude compared to the changes in the untreated *Gpx1*$^{-/-}$ mice. This is to be expected considering that *Sod1*$^{-/-}$ mice show a significant increase in oxidative damage under basal conditions compared to the *Gpx1*$^{-/-}$ mice (Figure 2B and 3B).

Similarity in gene expression between WT mice treated with diquat and untreated Sod1$^{-/-}$ mice points to a similar response to exogenous and endogenous oxidative stress

Because diquat and an absence of antioxidant enzymes are both expected to induce ~~an~~ overproduction of ROS, we compared the gene expression pattern induced by diquat in WT mice, ~~and~~ with that induced by the ablation of either Sod1 or Gpx1. We asked if changes in gene expression in either the *Sod1*$^{-/-}$ or *Gpx1*$^{-/-}$ mice were similar to the changes in gene expression caused by diquat treatment in WT mice at 3 to 6 h after diquat injection, which was the time interval when oxidative damage was maximal (Figures 2 and 3). Table V shows the number of genes that were significantly altered (in the same direction) in the untreated *Sod1*$^{-/-}$ or *Gpx1*$^{-/-}$ mice and in WT mice treated with diquat at the 3 or 6 h. As is shown in Table V, the changes in gene expression in WT mice treated with diquat are much more similar to the expression changes in untreated *Sod1*$^{-/-}$ mice than *Gpx1*$^{-/-}$ mice, which is especially true for highly upregulated genes. For example of the 321 genes upregulated more than 1.5-fold in WT mice treated with diquat, 26 were also upregulated more than 1.5-fold in the *Sod1*$^{-/-}$ mice. In contrast, only 2 out of 321 genes upregulated more than 1.5-fold in WT mice by diquat, were upregulated in the untreated *Gpx1*$^{-/-}$ mice. This comparison (from Table V) is presented graphically in Figure 4. The fold change of genes significantly altered by diquat at the either the 3 or 6 h time points (on the x-axis) was plotted against the fold change of the same genes also statistically significantly altered in the untreated *Gpx1*$^{-/-}$ or *Sod1*$^{-/-}$ mice (on the y-axis). A least-square regression line was then drawn through the data, with the slopes and R-square values given in Figure 4. A slope and R-square equal to one would be obtained if the gene expression changes in the two data sets were identical, while a value of zero for these parameters indicates no relationship between the data. As can be seen in Figure 4B and

D, the comparison of WT mice treated with diquat and *Gpx1*$^{-/-}$ mice yield a slope of the regression line and the R-square value very close to zero, as one would expect from randomly distributed data, indicating that the gene expression patterns between *Gpx1*$^{-/-}$ mice and WT mice treated with diquat were dissimilar. On the other hand (in Figure 4A and C), the comparison of *Sod1*$^{-/-}$ and WT mice treated with diquat, yielded a slope of 0.55 with an R-square of 0.54 ($P<0.001$) and a slope of 0.48 and an R-square of 0.41 ($P<0.001$) at the 3 h and 6 h time points, respectively. There ~~is~~ was little or no similarity in expression responses between diquat treatment and untreated *Gpx1*$^{-/-}$ mice, but a good degree of similarity between that caused by diquat treatment and the untreated *Sod1*$^{-/-}$ mice, which is in agreement with the fact that the *Sod1*$^{-/-}$ mice are oxidative stressed whereas the *Gpx1*$^{-/-}$ mice are not (Figures 2 and 3).

Identification of oxidative stress responsive transcripts

The major goal of this work was to find which genes are altered in response to oxidative stress *in vivo*. We screen our data for genes whose expression is responsive to oxidative stress by the following criteria: 1) they are altered by diquat in WT animals at the 3 or 6 h time interval (because oxidative damage peaks at these time points) and 2) they are altered in the untreated *Sod1*$^{-/-}$ mice, which already exhibit enhanced oxidative damage, though not in the *Gpx1*$^{-/-}$ mice, which do not exhibit increased oxidative damage (Figures 2 and 3). In other words, we asked what genes would be altered by exogenous as well as endogenous oxidative stress. As shown in Table V, a total of 121 transcripts met these criteria, with 37 transcripts being altered more than 1.5-fold (26 up, 11 down). The identities of these 37 transcripts are listed Table II (the discrepancy in the numbers between Table V and VI is because duplicate genes were deleted in VI). Alternatively, genes responsive to oxidative stress were selected in that they are altered by diquat in WT animals at the 3 or 6 h interval and are further altered significantly in the *Sod1*$^{-/-}$ or *Gpx1*$^{-/-}$ mice treated with diquat (i.e., the gene alterations in the *Sod1*$^{-/-}$ or *Gpx1*$^{-/-}$ mice at 1 h diquat treatment compared to WT after 1 h of diquat treatment, rows 4 and 2 in Webtable VI). In other words, we selected those genes that are hyper-inducible (or hyper-repressible) by diquat in the antioxidant knockout mice. A total of 188 transcripts met these criteria, with 21 being altered more than 2-fold (17 up, 4 down), and the identities of these 21 transcripts are given in Table III.

Validation of the microarray results

The changes in gene expression measured by microarrays were confirmed in two ways. First, we compared our data to previous studies where mRNA transcripts were measured by Northern blots. For example, we observed a dramatic (4- to 8-fold) increase in metallothionein 1 mRNA in the liver after diquat treatment or in *Sod1*$^{-/-}$ mice (Table II). Bauman *et al.* (5) reported a > 10-fold increase in metallothionein 1 mRNA levels in the livers of mice after diquat treatment, and Ghoshal *et al.* (26) and Levy *et al.* (52) have reported a >10-fold increase in metallothionein 1 mRNA levels in the liver of *Sod1*$^{-/-}$ mice. Because we performed experiments on *Sod1* and *Gpx1* knockout mice, it follows that the transcripts for *Sod1* and *Gpx1* should be very low or at the minimum, and that the region of the mRNA that corresponds to the exon that was targeted in the knockout should be either absent or highly downregulated as compared to the WT controls. In the *Sod1* knockout used in this study, exon 4 is deleted and exon 3 is truncated (41) but a mature mRNA is still expressed. Indeed, Affymetrix ID 1451124_at (which covers exon 3 and 4) was scored as “absent” in the 14 arrays in the *Sod1*$^{-/-}$, but as “present” in the 49 other arrays with wildtype *Sod1*; unfortunately, most of the values for this probeset were flagged as outliers by dChip (making it impossible to run all of the comparisons, which is why the squares are empty in the comparison group). The other probeset (Affymetrix id 1435304_at) covering the Sod1 gene was also scored as “absent” in the arrays covering *Sod1*$^{-/-}$ and decreased 1.41 fold, again, highly consistent with previous Northern blot data (41). The *Gpx1*$^{-/-}$ mice were made by targeting exon 2 with the neomycin resistance gene (34). Full

length mRNA *Gpx1* mRNA is not detectable; however, very low levels of a neomycin-gpx1 fusion mRNA are detectable after very long exposure (34). In full agreement with these known data, the probeset (Affymetrix ID 1460671_at) covering the *Gpx1* gene was decreased ~5 fold in the 14 arrays on the *Gpx1*$^{-/-}$ mice (34), and is in fact the most statistically significant alteration (in other words, with the lowest P value) in the *Gpx1*$^{-/-}$ mice regardless of the comparison.

Second, we used real time QRT-PCR to validate the expression of 5 genes: *Apoa4*, *Igfbp1*, *Pdk4*, and the p53-target genes *Cdkn1a* and *Gadd45a*. The expression of these genes were measured at 1, 3, 6, and 12 h after diquat treatment and in the untreated and diquat treated *Sod1*$^{-/-}$ and *Gpx1*$^{-/-}$ mice, i.e., we performed 39 comparisons (12 h diquat versus untreated WT comparison for Gadd45a was not available), and these data are shown in Webtable IV. In all samples, the transcripts for *Apoe4*, *Igfbp1*, *Pdk4*, *Cdkn1a* and *Gadd45a* readily amplified by QRT-PCR at the correct melting point. The array ratios of genes are validated when 95% confidence intervals for the QRT-PCR ratios overlap with the corresponding 95% confidence intervals for the array ratios. All values obtained by QRT-PCR overlapped with the microarray data at the 95% confidence interval, validating the microarray data we have obtained for these 5 genes at all the time points and mouse models.

Confirmation of selected transcripts at the protein level

We performed Western blot analyses to confirm selected mRNA upregulation at the protein level. In these experiments, we compared the protein levels in liver tissue from *Sod1*$^{-/-}$ vs. WT mice (Figures 5 and 6). From the genes in Table IV, we selected two highly upregulated transcripts (*Srxn1*, *Mt1*) and three modestly upregulated transcripts (*Txn2*, *Gpx4*, *Prdx1*) for Western blot confirmation. The two highly upregulated transcripts, *Mt1* and *Srxn1*, were also significantly upregulated at the protein level in the *Sod1*$^{-/-}$ mice (Figure 5). The *Srxn1* transcript was increased 2.3-fold and sulfiredoxin protein was increased more than 6-fold. The *Mt1* transcript was increased 4.5-fold and *Mt2* transcript was increased 3.6-fold (Webtable I) but the *Mt2* data did not reach the statistical cut-off ($p<0.0083$ vs. $p<0.005$); the protein levels of metallothionein 1+2 are increased 4.5-fold (Mt1 and 2 have the same molecular weight and the antibody does not distinguish between the two) in the liver of *Sod1*$^{-/-}$ mice. Out of the three modestly upregulated transcripts, only *Txn2* was also significantly upregulated (~2.5-fold) at the protein level (*Prdx1* and *Gpx4* were not, Figure 5). In addition, we confirmed the increase in the *Txnrd1* transcript by measuring thioredoxin reductase activity, which was increased by 90% in the cytosolic fraction of *Sod1*$^{-/-}$ mice. Because most of the upregulated antioxidant genes can be induced by *Nrf2* (see Discussion), we asked whether nuclear levels of *Nrf2* are increased in *Sod1*$^{-/-}$ as compared to WT mice (48). The nuclear levels of *Nrf2* were approximately 4-fold higher in *Sod1*$^{-/-}$ mice compared to WT mice (Figure 6A). We also performed Western blot analysis for two typical *Nrf2* target antioxidant genes that fell just below the statistical cut-off from the arrays (*Hmox1* and *Txn1*). Protein levels of heme oxygenase 1 (*Hmox1*) and thioredoxin 1 (*Txn1*) were significantly increased (2.3-fold and 50%, respectively). Because the upregulation of several p53-target genes suggested that alterations in p53 might be affected by oxidative stress, we measured the levels of p53 in the nucleus by Western blots. Nuclear levels of p53 were significantly elevated (30%) *Sod1*$^{-/-}$ mice compared to WT mice (Figure 6A). To confirm that the increase in p53 levels in the nucleus of *Sod1*$^{-/-}$ mice was due to higher activation of p53, we also measured the levels of phosphorylated p53 in total homogenate and nuclear factions obtained from the livers of *Sod1*$^{-/-}$ and WT mice. The nuclear levels of phosphorylated p53 were significantly higher (40%) compared to WT mice; however, we did not observed this effect when we examined p53 levels in the liver homogenates (Figure 6B). These data suggest that increased levels in p53 found in the nucleus of liver from *Sod1*$^{-/-}$ mice were due to an increase in the post-translational activation of p53 (phoshorylated) rather than an increase in the expression of p53.

DISCUSSION

To determine which changes in gene expression are most likely caused by oxidative stress we compared the expression patterns induced by diquat in WT mice with those of antioxidant knockout mice treated or untreated with diquat. In other words, we asked: Which genes would be altered by both exogenous and endogenous oxidative stress and which genes altered by diquat in WT animals would be enhanced by diquat in antioxidant knockout mice? We identified transcripts based on the following criteria: 1) they were altered by diquat in WT animals at 3 or 6 h after injection because oxidative damage peaks at that these time points (Table 2), 2) they were altered in untreated *Sod1*$^{-/-}$ mice, which have constitutively elevated oxidative damage (Table 2), and 3) they were altered to an even greater extent in the knockout mice, i.e., *Sod1*$^{-/-}$ or *Gpx1*$^{-/-}$ mice after diquat injection, i.e., transcripts that are hyper-inducible or hyper-repressible by diquat in antioxidant knockout mice (Table 3).

We initially expected that a large fraction of the transcripts that respond to increased oxidative stress would have antioxidant functions; however, the list of genes in Tables II and III are dominated by stress response genes. With the exception of metallothionein, none of these genes has any obvious antioxidant function. The pattern of gene expression changes we found to be induced consistently by oxidative stress *in vivo* was the upregulation of p53-target genes, many of which play a role in the genotoxic stress checkpoint response. In Table II (genes altered by both endogenous and exogenous oxidative stress), 6 out of 24 upregulated genes are p53-targets (44, 46): *Cdkn1a*/p21 (43, 64), *Gdf15* (40, 66), *Atf3* (56, 90), *Trp53inp1* (65, 81), *Ddit4* (23, 75) and *Ndrg1* (47, 79). While these genes were up-regulated in untreated *Sod1*$^{-/-}$ mice, none of them was upregulated in untreated *Gpx1*$^{-/-}$ mice, which is a control because the *Gpx1*$^{-/-}$ mice do not exhibit elevated oxidative damage. Two additional p53 transcriptional target genes, *Btg2* (12, 71) and *Plk3* (55, 89) are also in the list of genes in Table III; while a third, *Gadd45a* (36, 93), was not significantly induced in WT mice treated with diquat, but was significantly induced (<5-fold) in *Sod1*$^{-/-}$ mice treated with diquat (see Webtable I), suggesting this gene is responsive to oxidative stress, but only at very high levels of stress. *Btg2* and *Plk3* barely fell under the statistical cut-off in the untreated *Sod1*$^{-/-}$; on the other hand, the induction of these genes was dramatically higher in the *Sod1*$^{-/-}$ and *Gpx1*$^{-/-}$ mice treated with diquat as compared to WT treated with diquat (Table III).

p53 is normally present at very low levels in nucleus (or in the cell in general) because it is rapidly tagged for nuclear export and degradation, predominantly by *Mdm2* (37). Phosphorylation of p53 blocks the interaction with *Mdm2*, resulting in increased p53 half-life and increased levels in the nucleus where it initiates transcriptional activation of its targets. Therefore, we measured the levels of p53 and phospho-p53 in the nuclear fraction of WT and *Sod1*$^{-/-}$ mice to determine if the increased oxidative stress was correlated to the activation of p53. We found that the levels of p53 and phospho-p53 protein were significantly higher (30% to 40%) in nuclear fraction of the livers of *Sod1*$^{-/-}$ mice.

We compared our microarray results with a previous study from Prolla's laboratory (21) that reported gene expression changes induced *in vivo* in mouse heart by paraquat. Because paraquat and diquat are both bipyridil compounds that redox-cycle and generate superoxide (28,78), we aligned the arrays (updating the annotations in the process) to determine which genes were commonly altered in these two situations. Of the 228 genes significantly altered in heart by paraquat, 88 genes or 38% were also statistically altered by diquat in the liver (Webtable I). Tables II and III are annotated to indicate which gene alterations were also observed in paraquat-treated heart. Almost all the p53-target genes, which we identified in the present study, were also up-regulated in heart after paraquat treatment (21). Out of the nine p53-traget genes just mentioned (*Cdkn1a*/p21, *Gdf15*, *Atf3*, *Trp53inp1*, *Ddit4*, *Ndrg1*, *Btg2*, *Plk3*, *Gadd45a*), six were up-regulated by paraquat in the heart (re-analysis of Prolla's array indicates

that AI849939-unknown, induced >5-fold after paraquat injection, is *Ddit4*). *Trp53inp1* and *Plk3* were not present on Prolla's arrays while the probesets for *Gdf15* were of poor quality on the MG-U74A array. We also compared our data with the *in vitro* array data from Toledano's laboratory in which human cells [MCF7 breast cancerous and MRC9 lung fibroblasts (19)] were oxidatively stressed with a bolus dose of H_2O_2. Despite the experiments being conducted in different cell types, different species, different gene chips (of different gene composition), and different oxidative stressors, the following gene alterations were conserved: *p21*, *Gadd45a*, *Atf3*, *Btg2* and *Ddit4* are upregulated by a large magnitude *in vitro* in transformed MCF7 and normal MRC9 cells after H_2O_2 treatment [data from Table I in (19)], *in vivo* in heart following paraquat treatment (21), and in our present data set [regarding these comparisons, several of these genes appear under different synonyms in different papers, for example *Btg2* is also known as TIS21 or PC3 (71) and *Gdf15* is also known as PLAB]. Thus, the data indicate that the upregulation of p53 targets is a conserved response to oxidative stress across diverse organs and species.

The question arises as to whether the upregulation of p53 target genes is due to oxidative stress or arises as a consequence of massive cell damage triggering apoptosis. The microarray data do not support that the upregulation is involved in apoptosis because the classic p53 targets that are related to apoptosis, e.g., BAD, PUMA, NOXA [reviewed in (39)] were not significantly increased by diquat treatment in WT mice or in the untreated *Sod1*$^{-/-}$ mice, or even in the diquat treated *Sod1*$^{-/-}$ mice (Webtable I). The p53 targets genes that we observed to be oxidative stress responsive (e.g., p21, GADD45a, GDF15, Btg2) are predominantly involved in cell cycle arrest rather than apoptosis [reviewed in (92)].

While short-term oxidative stress induced by diquat treatment of WT, *Sod1*$^{-/-}$, and *Gpx1*$^{-/-}$ mice did not significantly induce the expression of the classical antioxidant enzymes (e.g., the superoxide dismutases, peroxiredoxins, glutaredoxins, catalases, glutathione reductases, or other glutathione peroxidases) in the livers of the mice, even though diquat treatment resulted in a dramatic increase in oxidative damage, long-term oxidative stress in the *Sod1*$^{-/-}$ mice did result in the significant upregulation of less well known antioxidant genes in untreated *Sod1*$^{-/-}$ mice compared to WT and *Gpx1*$^{-/-}$ mice (Table IV). As shown in Table IV, the most upregulated antioxidant gene was the small cysteine-rich protein, metallothionein 1 (~4.5-fold increase). Metallothionein 2 was also upregulated (~3.5-fold increase), but fell just below the statistical cut-off ($p<0.0083$ vs $p<0.005$). Using Western blots, we observed an ~5-fold increase in the levels of metallothionein 1 and 2. We also observed an ~2-fold increase in glutamate-cysteine ligase (*Gclc*) mRNA in the livers of *Sod1*$^{-/-}$ mice. Glutamate-cysteine ligase plays a critical role in the glutathione antioxidant system as the rate-limiting enzyme in glutathione biosynthesis (17,74). The upregulaton of *Gclc* is consistent with the observation by Marklund's group that levels of reduced glutathione (GSH) were increased in the livers of *Sod1*$^{-/-}$ mice (73). We also found several glutathione dependent enzymes to be upregulated (between 1.2-fold and 3-fold) in *Sod1*$^{-/-}$ mice, e.g., *Gpx4* and several glutathione-S-transferases, which exhibit glutathione peroxidase activity against fatty acid, lipid and organic hydroperoxides but not H_2O_2 (91). Lei *et al.* (51) recently reported an increase in overall glutathione-S-transferase enzymatic activity in the livers of *Sod1*$^{-/-}$ mice, which is in agreement with our array data. This same study also reported an ~50% increase in thioredoxin 1 reductase activity (51). We found that the *Trnxrd1* transcript was significantly upregulated in our arrays, and we also found that the activity of thioredoxin reductase was also significantly increased (~90%) in the livers of the *Sod1*$^{-/-}$ mice. The transcript of selenoprotein W was also found to be significantly increased 45% in the liver of *Sod1*$^{-/-}$ mice. Selenoprotein W is a small glutathione interacting protein (7), whose exact function is unknown; however, it appears to have antioxidant properties and is also upregulated in the liver during cadmium oxidative stress (86). When ectopically expressed in cell culture, selenoprotein W provides protection against hydrogen peroxide (42). Perhaps most interesting of all changes in gene expression in the livers of

Sod1$^{-/-}$ mice was the >2-fold upregulation of the sulfiredoxin (*Srxn1*) transcript and the 6-fold increase in sulfiredoxin protein. Sulfiredoxin was identified in yeast as an enzyme that is capable of reversing what was previously thought to be irreversibly oxidative modification of cysteine [i.e., sulfinic acid, (10)]. Our study is the first to demonstrate a direct association between oxidative stress and elevation in sulfiredoxin expression in mammals.

The common thread in these observations is a concerted upregulation of the thiol antioxidant system (metallothione, glutathione, thioredoxin, sulfiredoxin) and its associated enzymes in the *Sod1*$^{-/-}$ liver. The upregulation of so many components of the thiol antioxidant system in the *Sod1*$^{-/-}$ liver could be physiologically protective because free thiols react with superoxide at ~10^3 to ~10^4 M^{-1} s^{-1} (9,87), thereby scavenging the excess superoxide in the absence of CuZnSOD. Thiol antioxidants, e.g., glutathione, Nacetyl cysteine, cysteine, and metallothionein can rescue *Sod1*$^{-/-}$ yeast (80,94) and elevated glutathione biosynthesis rescues neuroblastoma cells in which CuZnSOD was knocked down by RNAi (2). Of the antioxidant genes upregulated in the *Sod1*$^{-/-}$ listed in Table IV, none were statistically significantly altered in the *Gpx1*$^{-/-}$ mice, which exhibit no significant elevation in oxidative damage in the absence of exogenous oxidative stressors.

Many of the antioxidant genes altered in the livers of *Sod1*$^{-/-}$ mice (listed in Table IV) are known to be under the control of the transcription factor, *Nrf2* [e.g., glutathione-S transferases, sulfiredoxin, glutamate cysteine ligase, and thioredoxin reductase 1 (48)]. *Nrf2* is normally sequestered in the cytoplasm by its binding partner *Keap1*. When the *Keap1* is oxidized, *Nrf2* is activated and transitions to the nucleus to induce the transcription of its target genes (48,86). We observed no significant change in the *Nrf2* transcript in our array data. However, the level of *Nrf2* protein in the nuclear fraction of the liver of *Sod1*$^{-/-}$ mice was increased ~4.5-fold compared to WT mice, which is consistent oxidative stress inducing the transcription of glutathione-S transferases, sulfiredoxin, glutamate cysteine ligase, and thioredoxin reductase 1 through the activation of *Nrf2*.

In conclusion, the expression response to elevated oxidative stress *in vivo* does not constitute an upregulation of classical antioxidant genes, although long-term oxidative stress in the *Sod1*$^{-/-}$ mice leads to a significant upregulation of thiol antioxidants. Rather, we found that an upregulation of p53 target genes was a common and robust feature of oxidative stress *in vivo*. Our retrospective review of the literature shows that an upregulation in p53 target genes is a conserved expression response to oxidative stress across different organs and species, and holds true *in vitro* and *in vivo*. Thus, our study points to p53 playing an important role in the induction of gene expression in response to oxidative stress.

REFERENCES

1. Amador-Noguez D, Yagi K, Venable S, Darlington G. Gene expression profile of long-lived Ames dwarf mice and Little mice. Aging Cell 2004;3:423–441. [PubMed: 15569359]
2. Aquilano K, Vigilanza P, Rotilio G, Ciriolo MR. Mitochondrial damage due to SOD1 deficiency in SH-SY5Y neuroblastoma cells: a rationale for the redundancy of SOD1. Faseb J 2006;20:1683–1685. [PubMed: 16790527]
3. Awad JA, Burk RF, Roberts LJ 2nd. Effect of selenium deficiency and glutathione-modulating agents on diquat toxicity and lipid peroxidation in rats. J Pharmacol Exp Ther 1994;270:858–864. [PubMed: 7932197]
4. Baranano DE, Rao M, Ferris CD, Snyder SH. Biliverdin reductase: a major physiologic cytoprotectant. Proc Natl Acad Sci U S A 2002;99:16093–16098. [PubMed: 12456881]
5. Bauman JW, Liu J, Liu YP, Klaassen CD. Increase in metallothionein produced by chemicals that induce oxidative stress. Toxicol Appl Pharmacol 1991;110:347–354. [PubMed: 1891778]
6. Beckman KB, Ames BN. The free radical theory of aging matures. Physiol Rev 78:547–1998. [PubMed: 9562038]

7. Beilstein MA, Vendeland SC, Barofsky E, Jensen ON, Whanger PD. Selenoprotein W of rat muscle binds glutathione and an unknown small molecular weight moiety. J Inorg Biochem 1996;61:117–124. [PubMed: 8576706]
8. Bernal J, Coleoni AH, DeGroot LJ. Triiodothyronine stimulation of nuclear protein synthesis. Endocrinology 1978;102:452–459. [PubMed: 743968]
9. Bielski BH, Arudi RL, Sutherland MW. A study of the reactivity of $HO_2^{\cdot}/O_2^{\cdot -}$ with unsaturated fatty acids. Journal of Biological Chemistry 1983;258:4759–4761. [PubMed: 6833274]
10. Biteau B, Labarre J, Toledano MB. ATP-dependent reduction of cysteinesulphinic acid by S. cerevisiae sulphiredoxin. Nature 2003;425:980–984. [PubMed: 14586471]
11. Blander G, de Oliveira RM, Conboy CM, Haigis M, Guarente L. Superoxide dismutase 1 knock-down induces senescence in human fibroblasts. J Biol Chem 2003;278:38966–38969. [PubMed: 12871978]
12. Boiko AD, Porteous S, Razorenova OV, Krivokrysenko VI, Williams BR, Gudkov AV. A systematic search for downstream mediators of tumor suppressor function of p53 reveals a major role of BTG2 in suppression of Ras-induced transformation. Genes Dev 2006;20:236–252. [PubMed: 16418486]
13. Busuttil RA, Rubio M, Dolle ME, Campisi J, Vijg J. Oxygen accelerates the accumulation of mutations during the senescence and immortalization of murine cells in culture. Aging Cell 2003;2:287–294. [PubMed: 14677631]
14. Chance B, Sies H, Boveris A. Hydroperoxide metabolism in mammalian organs. Physiol Rev 1979;59:527–605. [PubMed: 37532]
15. Coleoni AH, DeGroot LJ. Liver nuclear protein phosphorylation in vivo and the effect of triiodothyronine. Endocrinology 1980;106:1103–1107. [PubMed: 7358026]
16. Cook P, Fu C, Hickey M, Han ES, Miller KS. SAS programs for real-time RTPCR having multiple independent samples. Biotechniques 2004;37:990–995. [PubMed: 15597549]
17. Dalton TP, Dieter MZ, Yang Y, Shertzer HG, Nebert DW. Knockout of the mouse glutamate cysteine ligase catalytic subunit (Gclc) gene: embryonic lethal when homozygous, and proposed model for moderate glutathione deficiency when heterozygous. Biochem Biophys Res Commun 2000;279:324–329. [PubMed: 11118286]
18. Dandrea T, Hellmold H, Jonsson C, Zhivotovsky B, Hofer T, Warngard L, Cotgreave I. The transcriptosomal response of human A549 lung cells to a hydrogen peroxide-generating system: relationship to DNA damage, cell cycle arrest, and caspase activation. Free Radic Biol Med 2004;36:881–896. [PubMed: 15019973]
19. Desaint S, Luriau S, Aude JC, Rousselet G, Toledano MB. Mammalian antioxidant defenses are not inducible by H2O. J Biol Chem 2004;279:31157–31163. [PubMed: 15155764]
20. Duttaroy A, Paul A, Kundu M, Belton A. A Sod2 null mutation confers severely reduced adult life span in Drosophila. Genetics 2003;165:2295–2299. [PubMed: 14704205]
21. Edwards MG, Sarkar D, Klopp R, Morrow JD, Weindruch R, Prolla TA. Age-related impairment of the transcriptional responses to oxidative stress in the mouse heart. Physiol Genomics 2003;13:119–127. [PubMed: 12595580]
22. Elchuri S, Oberley TD, Qi W, Eisenstein RS, Jackson Roberts L, Van Remmen H, Epstein CJ, Huang TT. CuZnSOD deficiency leads to persistent and widespread oxidative damage and hepatocarcinogenesis later in life. Oncogene 2005;24:367–380. [PubMed: 15531919]
23. Ellisen LW, Ramsayer KD, Johannessen CM, Yang A, Beppu H, Minda K, Oliner JD, McKeon F, Haber DA. REDD1, a developmentally regulated transcriptional target of p63 and p53, links p63 to regulation of reactive oxygen species. Mol Cell 2002;10:995–1005. [PubMed: 12453409]
24. Finkel T. Reactive oxygen species and signal transduction. IUBMB Life 2001;52:3–6. [PubMed: 11795590]
25. Fu C, Xi L, Wu Y, McCarter R, Richardson A, Hickey M, Han ES. Hepatic genes altered in expression by food restriction are not influenced by the low plasma glucose level in young male GLUT4 transgenic mice. J Nutr 2004;134:2965–2974. [PubMed: 15514260]
26. Ghoshal K, Majumder S, Li Z, Bray TM, Jacob ST. Transcriptional induction of metallothionein-I and -II genes in the livers of Cu, Zn-superoxide dismutase knockout mice. Biochem Biophys Res Commun 1999;264:735–742. [PubMed: 10544001]

27. Gromer S, Merkle H, Schirmer RH, Becker K. Human placenta thioredoxin reductase: preparation and inhibitor studies. Methods Enzymol 2002;347:382–394. [PubMed: 11898429]
28. Halliwell, B.; Gutteridge, J. Free radicals in Biology and Medicine. Vol. 1999. New York: Oxford University Press;
29. Hamilton ML, Guo Z, Fuller CD, Van Remmen H, Ward WF, Austad SN, Troyer DA, Thompson I, Richardson A. A reliable assessment of 8-oxo-2-deoxyguanosine levels in nuclear and mitochondrial DNA using the sodium iodide method to isolate DNA. Nucleic Acids Res 2001;29:2117–2126. [PubMed: 11353081]
30. Hamilton ML, Van Remmen H, Drake JA, Yang H, Guo ZM, Kewitt K, Walter CA, Richardson A. Does oxidative damage to DNA increase with age? Proc Natl Acad Sci U S A 2001;98:10469–10474. [PubMed: 11517304]
31. Han ES, Wu Y, McCarter R, Nelson JF, Richardson A, Hilsenbeck SG. Reproducibility, sources of variability, pooling, and sample size: important considerations for the design of high-density oligonucleotide array experiments. J Gerontol A Biol Sci Med Sci 2004;59:306–315. [PubMed: 15071073]
32. Harman D. Aging: A theory based on free radical and radiation chemistry. Journal of Gerontology 1956;11:298–300. [PubMed: 13332224]
33. Hassan HM, Fridovich I. Superoxide radical and the oxygen enhancement of the toxicity of paraquat in Escherichia coli. J Biol Chem 1978;253:8143–8148. [PubMed: 213429]
34. Ho YS, Magnenat JL, Bronson RT, Cao J, Gargano M, Sugawara M, Funk CD. Mice deficient in cellular glutathione peroxidase develop normally and show no increased sensitivity to hyperoxia. J Biol Chem 1997;272:16644–16651. [PubMed: 9195979]
35. Hochberg Y, Benjamini Y. More powerful procedures for multiple significance testing. Stat Med 1990;9:811–818. [PubMed: 2218183]
36. Hollander MC, Sheikh MS, Bulavin DV, Lundgren K, Augeri-Henmueller L, Shehee R, Molinaro TA, Kim KE, Tolosa E, Ashwell JD, Rosenberg MP, Zhan Q, Fernandez-Salguero PM, Morgan WF, Deng CX, Fornace AJ Jr. Genomic instability in Gadd45a-deficient mice. Nat Genet 1999;23:176–184. [PubMed: 10508513]
37. Horn HF, Vousden KH. Coping with stress: multiple ways to activate p53. Oncogene 2007;26:1306–1316. [PubMed: 17322916]
38. Hornsby PJ. Mouse and human cells versus oxygen. Sci Aging Knowledge Environ 2003;2003:PE21. [PubMed: 12890857]
39. Horvath MM, Wang X, Resnick MA, Bell DA. Divergent evolution of human p53 binding sites: cell cycle versus apoptosis. PLoS Genet 2007;3:e127. [PubMed: 17677004]
40. Hsiao EC, Koniaris LG, Zimmers-Koniaris T, Sebald SM, Huynh TV, Lee SJ. Characterization of growth-differentiation factor 15, a transforming growth factor beta superfamily member induced following liver injury. Mol Cell Biol 2000;20:3742–3751. [PubMed: 10779363]
41. Huang TT, Yasunami M, Carlson EJ, Gillespie AM, Reaume AG, Hoffman EK, Chan PH, Scott RW, Epstein CJ. Superoxide-mediated cytotoxicity in superoxide dismutase-deficient fetal fibroblasts. Arch Biochem Biophys 1997;344:424–432. [PubMed: 9264557]
42. Jeong D, Kim TS, Chung YW, Lee BJ, Kim IY. Selenoprotein W is a glutathionedependent antioxidant in vivo. FEBS Lett 2002;517:225–228. [PubMed: 12062442]
43. Johnson M, Dimitrov D, Vojta PJ, Barrett JC, Noda A, Pereira-Smith OM, Smith JR. Evidence for a p53-independent pathway for upregulation of SDI1/CIP1/WAF1/p21 RNA in human cells. Mol Carcinog 1994;11:59–64. [PubMed: 7522462]
44. Kannan K, Amariglio N, Rechavi G, Jakob-Hirsch J, Kela I, Kaminski N, Getz G, Domany E, Givol D. DNA microarrays identification of primary and secondary target genes regulated by p53. Oncogene 2001;20:2225–2234. [PubMed: 11402317]
45. Kehrer JP, Haschek WM, Witschi H. The influence of hyperoxia on the acute toxicity of paraquat and diquat. Drug Chem Toxicol 1979;2:397–408. [PubMed: 540539]
46. Kho PS, Wang Z, Zhuang L, Li Y, Chew JL, Ng HH, Liu ET, Yu Q. p53-regulated transcriptional program associated with genotoxic stress-induced apoptosis. J Biol Chem 2004;279:21183–21192. [PubMed: 15016801]

47. Kokame K, Kato H, Miyata T. Homocysteine-respondent genes in vascular endothelial cells identified by differential display analysis. GRP78/BiP and novel genes. J Biol Chem 1996;271:29659–29665. [PubMed: 8939898]
48. Kwak MK, Wakabayashi N, Itoh K, Motohashi H, Yamamoto M, Kensler TW. Modulation of gene expression by cancer chemopreventive dithiolethiones through the Keap1-Nrf2 pathway. Identification of novel gene clusters for cell survival. J Biol Chem 2003;278:8135–8145.
49. Lebovitz RM, Zhang H, Vogel H, Cartwright J, Dionne L, Lu N, Huang S, Matzuk MM. Neurodegeneration, myocardial injury, and perinatal death in mitochondrial superoxide dismutase-deficient mice. Proc Natl Acad Sci U S A 1996;93:9782–9787. [PubMed: 8790408]
50. Lee TH, Kim SU, Yu SL, Kim SH, Park do S, Moon HB, Dho SH, Kwon KS, Han YH, Jeong S, Kang SW, Shin HS, Lee KK, Rhee SG, Yu DY. Peroxiredoxin II is essential for sustaining life span of erythrocytes in mice. Blood 2003;101:5033–5038. [PubMed: 12586629]
51. Lei XG, Zhu JH, McClung JP, Aregullin M, Roneker CA. Mice deficient in Cu, Zn-superoxide dismutase are resistant to acetaminophen toxicity. Biochem J. 2006
52. Levy MA, Tsai YH, Reaume A, Bray TM. Cellular response of antioxidant metalloproteins in Cu/Zn SOD transgenic mice exposed to hyperoxia. Am J Physiol Lung Cell Mol Physiol 2001;281:172–182.
53. Li C, Wong WH. Model-based analysis of oligonucleotide arrays: expression index computation and outlier detection. Proc Natl Acad Sci U S A 2001;98:31–36. [PubMed: 11134512]
54. Li Y, Huang TT, Carlson EJ, Melov S, Ursell PC, Olson JL, Noble LJ, Berger C, Chan PH, et al. Dilated cardiomyopathy and neonatal lethality in mutant mice lacking manganese superoxide dismutase. Nat Genet 1995;11:376–381. [PubMed: 7493016]
55. Li Z, Niu J, Uwagawa T, Peng B, Chiao PJ. Function of polo-like kinase 3 in NFkappaB-mediated proapoptotic response. J Biol Chem 2005;280:16843–16850. [PubMed: 15671037]
56. Liang G, Wolfgang CD, Chen BP, Chen TH, Hai T. ATF3 gene. Genomic organization, promoter, and regulation. J Biol Chem 1996;271:1695–1701. [PubMed: 8576171]
57. Marklund SL. Human copper-containing superoxide dismutase of high molecular weight. Proc Natl Acad Sci U S A 1982;79:7634–7638. [PubMed: 6961438]
58. McCord JM, Fridovich I. Superoxide dismutase. An enzymic function for erythrocuprein (hemocuprein). Journal of Biological Chemistry 1969;244:6049–6055. [PubMed: 5389100]
59. Morrow JD, Awad JA, Boss HJ, Blair IA, Roberts LJ 2nd. Noncyclooxygenase-derived prostanoids (F2-isoprostanes) are formed in situ on phospholipids. Proc Natl Acad Sci U S A 1992;89:10721–10725. [PubMed: 1438268]
60. Morrow JD, Hill KE, Burk RF, Nammour TM, Badr KF, Roberts LJ 2nd. A series of prostaglandin F2-like compounds are produced in vivo in humans by a noncyclooxygenase, free radical-catalyzed mechanism. Proc Natl Acad Sci U S A 1990;87:9383–9387. [PubMed: 2123555]
61. Muller F. The Nature and Mechanism of Superoxide production by the Electron Transport Chain: Its relevance to aging. J Amer Aging Assoc 2000;23:227–253.
62. Muller, FL.; Mele, J.; Van Remmen, H.; Richardson, A. Probing the *In Vivo* Relevance of Oxidative Stress in Aging Using Knockout and Transgenic Mice. In: Von Zglinicki, T., editor. Aging at the Molecular Level. Kluwer Academic Publishers; 2003. p. 131-144.
63. Neumann CA, Krause DS, Carman CV, Das S, Dubey DP, Abraham JL, Bronson RT, Fujiwara Y, Orkin SH, Van Etten RA. Essential role for the peroxiredoxin Prdx1 in erythrocyte antioxidant defence and tumour suppression. Nature 2003;424:561–565. [PubMed: 12891360]
64. Noda A, Ning Y, Venable SF, Pereira-Smith OM, Smith JR. Cloning of senescent cell-derived inhibitors of DNA synthesis using an expression screen. Exp Cell Res 1994;211:90–98. [PubMed: 8125163]
65. Okamura S, Arakawa H, Tanaka T, Nakanishi H, Ng CC, Taya Y, Monden M, Nakamura Y. p53DINP1, a p53-inducible gene, regulates p53-dependent apoptosis. Mol Cell 2001;8:85–94. [PubMed: 11511362]
66. Paralkar VM, Vail AL, Grasser WA, Brown TA, Xu H, Vukicevic S, Ke HZ, Qi H, Owen TA, Thompson DD. Cloning and characterization of a novel member of the transforming growth factor-beta/bone morphogenetic protein family. J Biol Chem 1998;273:13760–13767. [PubMed: 9593718]

67. Parrinello S, Samper E, Krtolica A, Goldstein J, Melov S, Campisi J. Oxygen sensitivity severely limits the replicative lifespan of murine fibroblasts. Nat Cell Biol 2003;5:741–747. [PubMed: 12855956]
68. Pratt IS, Keeling PL, Smith LL. The effect of high concentrations of oxygen on paraquat and diquat toxicity in rats. Arch Toxicol Suppl 1980;4:415–418. [PubMed: 6933951]
69. Reitman S, Frankel S. A colorimetric method for the determination of serum glutamic oxalacetic and glutamic pyruvic transaminases. Am J Clin Pathol 1957;28:56–63. [PubMed: 13458125]
70. Rhodes ML, Zavala DC, Brown D. Hypoxic protection in paraquat poisoning. Lab Invest 1976;35:496–500. [PubMed: 994461]
71. Rouault JP, Falette N, Guehenneux F, Guillot C, Rimokh R, Wang Q, Berthet C, Moyret-Lalle C, Savatier P, Pain B, Shaw P, Berger R, Samarut J, Magaud JP, Ozturk M, Samarut C, Puisieux A. Identification of BTG2, an antiproliferative p53-dependent component of the DNA damage cellular response pathway. Nat Genet 1996;14:482–486. [PubMed: 8944033]
72. Sambrook, J.; Maniatis, T.; Fritsch, EF. Sambrook, J.; Maniatis, T.; Fritsch, EF. Molecular Cloning A Laboratory Manual. Cold Spring Harbor; 1982. Extraction, purification, and analysis of mRNA from eukaryotic cells; p. 196
73. Sentman ML, Granstrom M, Jakobson H, Reaume A, Basu S, Marklund SL. Phenotypes of mice lacking extracellular superoxide dismutase and copper- and zinc-containing superoxide dismutase. J Biol Chem 2006;281:6904–6909. [PubMed: 16377630]
74. Shi ZZ, Osei-Frimpong J, Kala G, Kala SV, Barrios RJ, Habib GM, Lukin DJ, Danney CM, Matzuk MM, Lieberman MW. Glutathione synthesis is essential for mouse development but not for cell growth in culture. Proc Natl Acad Sci U S A 2000;97:5101–5106. [PubMed: 10805773]
75. Shoshani T, Faerman A, Mett I, Zelin E, Tenne T, Gorodin S, Moshel Y, Elbaz S, Budanov A, Chajut A, Kalinski H, Kamer I, Rozen A, Mor O, Keshet E, Leshkowitz D, Einat P, Skaliter R, Feinstein E. Identification of a novel hypoxia-inducible factor 1-responsive gene, RTP801, involved in apoptosis. Mol Cell Biol 2002;22:2283–2293. [PubMed: 11884613]
76. Smith LL. Mechanism of paraquat toxicity in lung and its relevance to treatment. Hum Toxicol 1987;6:31–36. [PubMed: 3546084]
77. Stadtman ER. Protein oxidation in aging and age-related diseases. Ann N Y Acad Sci 2001;928:22–38. [PubMed: 11795513]
78. Stancliffe TC, Pirie A. The production of superoxide radicals in reactions of the herbicide diquat. FEBS Lett 1971;17:297–299. [PubMed: 11946050]
79. Stein S, Thomas EK, Herzog B, Westfall MD, Rocheleau JV, Jackson RS 2nd, Wang M, Liang P. NDRG1 is necessary for p53-dependent apoptosis. J Biol Chem 2004;279:48930–48940. [PubMed: 15377670]
80. Tamai KT, Gralla EB, Ellerby LM, Valentine JS, Thiele DJ. Yeast and mammalian metallothioneins functionally substitute for yeast copper-zinc superoxide dismutase. Proc Natl Acad Sci U S A 1993;90:8013–8017. [PubMed: 8367458]
81. Tomasini R, Samir AA, Pebusque MJ, Calvo EL, Totaro S, Dagorn JC, Dusetti NJ, Iovanna JL. P53-dependent expression of the stress-induced protein (SIP). Eur J Cell Biol 2002;81:294–301. [PubMed: 12067065]
82. Van Remmen H, Richardson A. Oxidative damage to mitochondria and aging. Exp Gerontol 2001;36:957–968. [PubMed: 11404044]
83. Wang X, Phelan SA, Forsman-Semb K, Taylor EF, Petros C, Brown A, Lerner CP, Paigen B. Mice with targeted mutation of peroxiredoxin 6 develop normally but are susceptible to oxidative stress. J Biol Chem 2003;278:25179–25190. [PubMed: 12732627]
84. Ward WF, Qi W, Van Remmen H, Zackert WE, Roberts LJ 2nd, Richardson A. Effects of age and caloric restriction on lipid peroxidation: measurement of oxidative stress by F2-isoprostane levels. J Gerontol A Biol Sci Med Sci 2005;60:847–851. [PubMed: 16079206]
85. Weisiger RA, Fridovich I. Mitochondrial superoxide simutase. Site of synthesis and intramitochondrial localization. J Biol Chem 1973;248:4793–4796. [PubMed: 4578091]
86. Wimmer U, Wang Y, Georgiev O, Schaffner W. Two major branches of anticadmium defense in the mouse: MTF-1/metallothioneins and glutathione. Nucleic Acids Res 2005;33:5715–5727. [PubMed: 16221973]

87. Winterbourn CC, Metodiewa D. Reactivity of biologically important thiol compounds with superoxide and hydrogen peroxide. Free Radic Biol Med 1999;27:322–328. [PubMed: 10468205]

88. Wood ZA, Schroder E, Robin Harris J, Poole LB. Structure, mechanism and regulation of peroxiredoxins. Trends Biochem Sci 2003;28:32–40. [PubMed: 12517450]

89. Xie S, Wang Q, Wu H, Cogswell J, Lu L, Jhanwar-Uniyal M, Dai W. Reactive oxygen species-induced phosphorylation of p53 on serine 20 is mediated in part by polo-like kinase. J Biol Chem 2001;276:36194–36199. [PubMed: 11447225]

90. Yan C, Lu D, Hai T, Boyd DD. Activating transcription factor 3, a stress sensor, activates p53 by blocking its ubiquitination. Embo J 2005;24:2425–2435. [PubMed: 15933712]

91. Yant LJ, Ran Q, Rao L, Van Remmen H, Shibatani T, Belter JG, Motta L, Richardson A, Prolla TA. The selenoprotein GPX4 is essential for mouse development and protects from radiation and oxidative damage insults. Free Radic Biol Med 2003;34:496–502. [PubMed: 12566075]

92. Yu J, Zhang L. The transcriptional targets of p53 in apoptosis control. Biochem Biophys Res Commun 2005;331:851–858. [PubMed: 15865941]

93. Zhan Q, Bae I, Kastan MB, Fornace AJ Jr. The p53-dependent gamma-ray response of GADD45. Cancer Res 1994;54:2755–2760. [PubMed: 8168107]

94. Zyracka E, Zadrag R, Koziol S, Krzepilko A, Bartosz G, Bilinski T. Yeast as a biosensor for antioxidants: simple growth tests employing a Saccharomyces cerevisiae mutant defective in superoxide dismutase. Acta Biochim Pol 2005;52:679–684. [PubMed: 16175242]

Supplementary Material

Refer to Web version on PubMed Central for supplementary material.

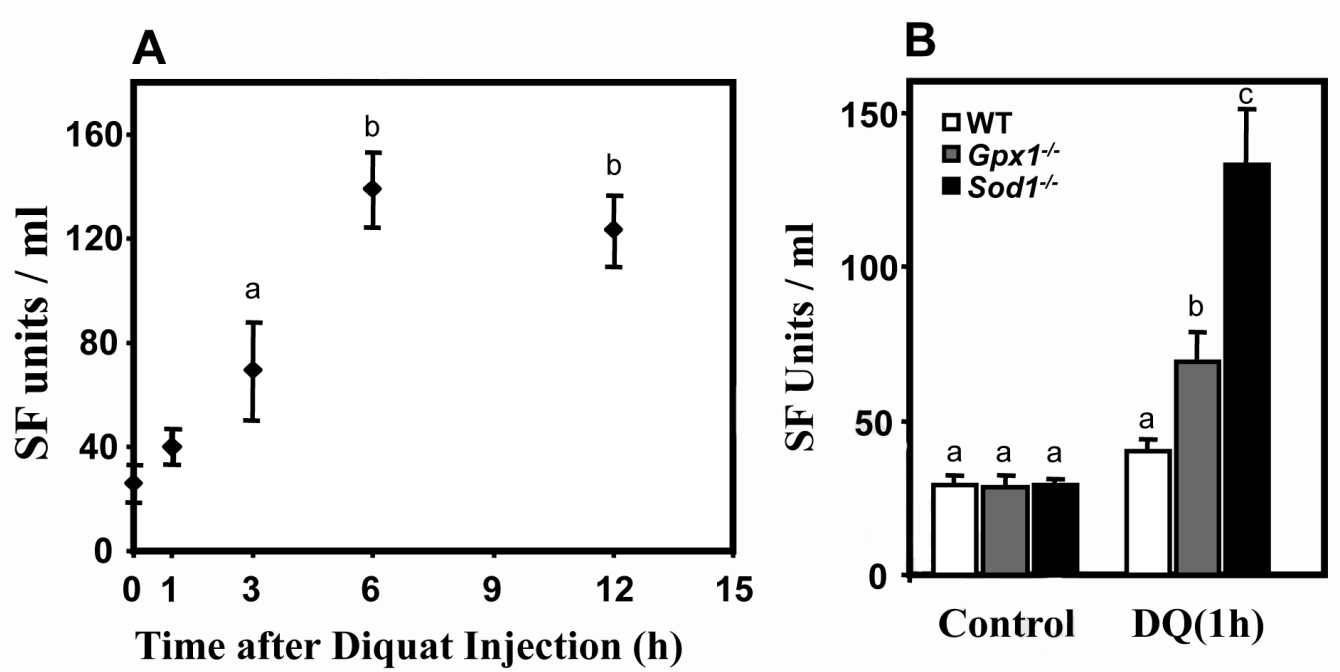

Figure 1. Liver injury induced by diquat is greater in mice lacking either SOD1 or GPX1

Hepatotoxicity of a single dose of diquat (50 mg/kg body weight given i.p.) was measured by the plasma ALT activity as described in the Experimental Procedures. **Graph A:** The levels of plasma ALT activity are shown at various times after diquat administration for WT mice. Each point represents the mean ± S.E.M. of data collected from 3 mice. Values with different letter superscripts are significantly different from each other and from the control and 1 h values at the $p<0.05$ level. **Graph B:** The effect of genotype and diquat treatment on plasma ALT activity. Plasma ALT activities of WT (open bars), *Gpx1*$^{-/-}$ (shaded bars), and *Sod1*$^{-/-}$ (black bars) mice were determined in untreated mice and 1 h after diquat treatment. Each bar represents the mean ± S.E.M. of data from 5 mice. Values with different letter superscripts are significantly different from each other at the $p<0.05$ level.

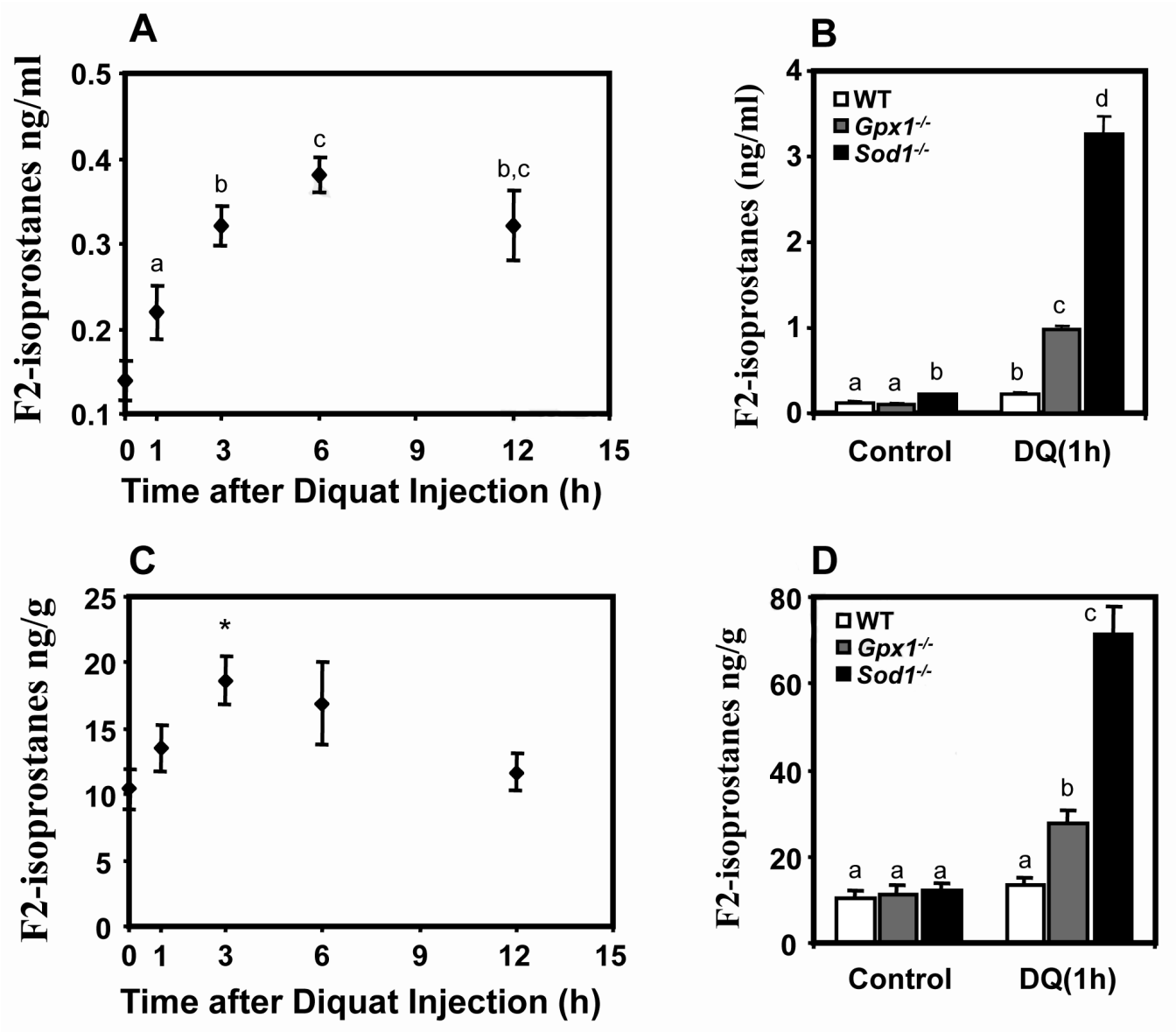

Figure 2. Lipid peroxidation induced by diquat is greater in antioxidant enzyme deficient mice

Plasma and liver tissue were collected at the indicated time after diquat treatment. The levels of F_2-isoprostanes from plasma and liver were determined as described in the Experimental Procedures. The levels of F_2-isoprostanes are expressed as ng per ml serum or per g of tissue for isoprostane in plasma and liver, respectively. **Graphs A and B:** The levels of free F_2-isoprostanes were measured in the plasma in WT mice at various times after diquat administration (**A**) or in the plasma of WT (open bars), *Gpx1*$^{-/-}$ (shaded bars), and *Sod1*$^{-/-}$ (black bars) untreated mice and 1 h after diquat treatment (**B**). Plasma was pooled from 3 mice, and each value represents the mean ± S.E.M. of data from 3 pooled samples (9 mice total). Values with different letter superscripts are significantly different from each other at the $p<0.05$ level. **Graphs C and D:** The levels of esterfied F_2-isoprostanes were measured in the livers in WT mice at various times after diquat administration (**C**) or in the livers of WT (open bars), *Gpx1*$^{-/-}$(shaded bars), and *Sod1*$^{-/-}$ (black bars) untreated mice and 1 h after diquat treatment (**D**). Each value represents the mean ± S.E.M. of data from 4 mice. The "*" indicates a value that is significantly different ($p<0.05$ level) from untreated mice and mice 12 h after diquat

treatment. Values with different letter superscripts are significantly different from each other at the $p<0.05$ level.

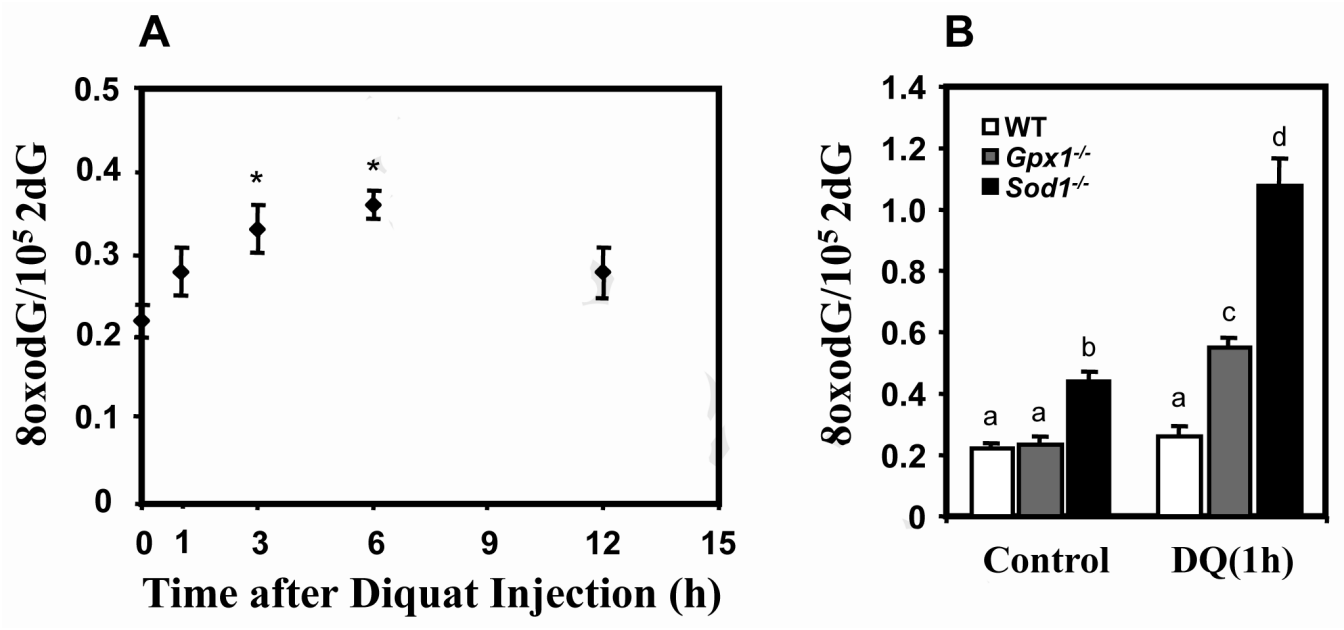

Figure 3. Effect of antioxidant enzyme deficiency on diquat-induced DNA oxidation

Nuclear DNA was isolated from liver tissue collected at the indicated time after diquat injection and DNA oxidation was measured as described in the Experimental Procedures and expressed as a ratio nmol of 8-oxo-dG to 10^5nmol of 2-dG. **Graph A:** The time course of DNA oxidation induced by diquat treatment is shown at various times after diquat administration for WT mice. Each point represents the mean ± S.E.M. of data collected from 4 mice. The "*" indicates values that are significantly different ($p<0.05$) from untreated mice. **Graph B:** DNA oxidation was measured in the livers of WT (open bars), $Gpx1^{-/-}$(shaded bars), and $Sod1^{-/-}$ (black bars) mice before and 1 h after diquat treatment. Each bar represents the mean ± S.E.M. of data from 4 mice. Values with different letter superscripts are significantly different from each other at the $p<0.05$ level.

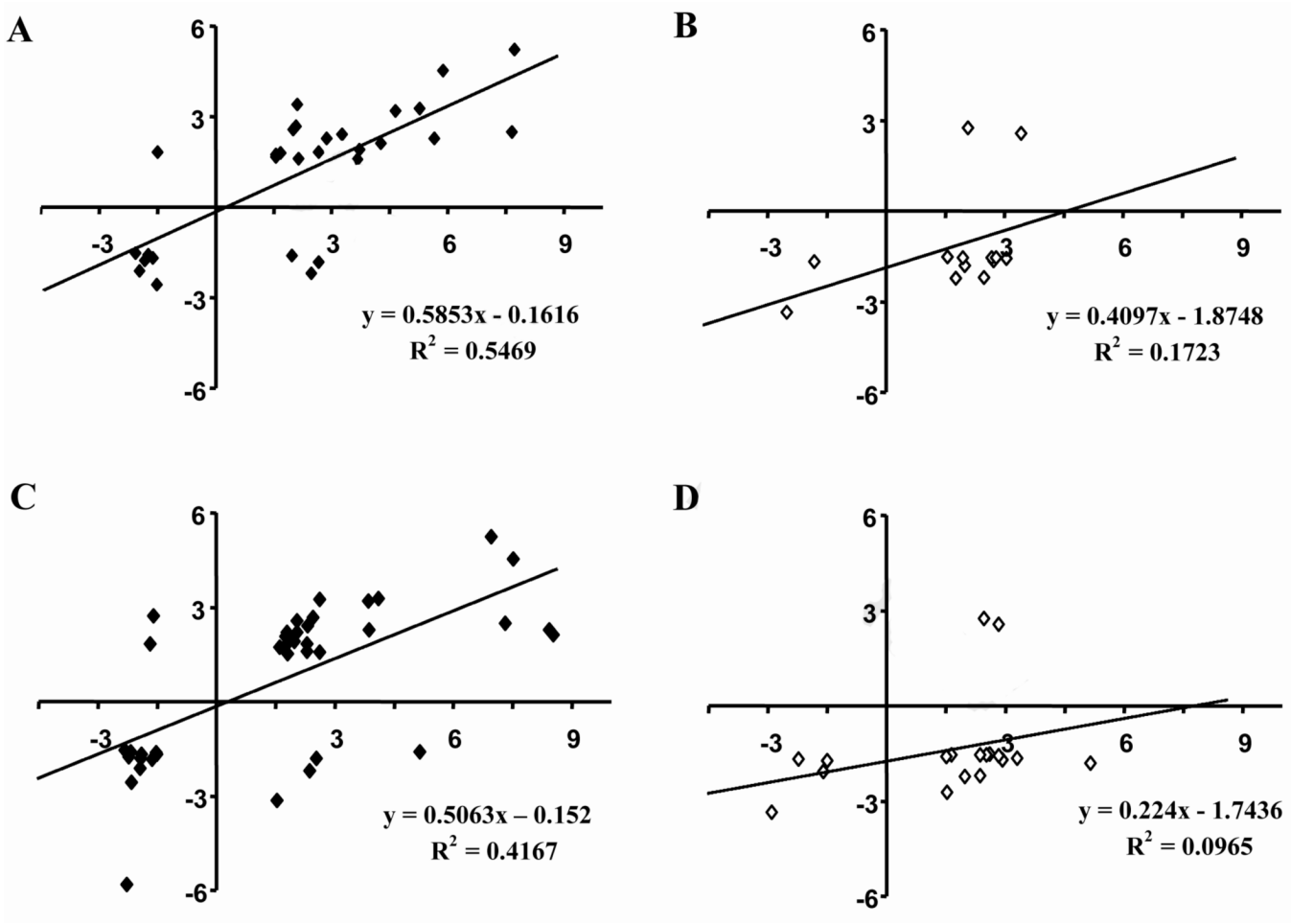

Figure 4. The expression pattern elicited by diquat in WT mice is similar to that of the untreated Sod1$^{-/-}$ animals

The fold-change (all fold changes are in comparison to untreated WT control) of genes significantly altered (P<0.005) both by diquat in WT animals (at the 3 or 6 h time points) and in untreated antioxidant knockout mice was determined, and the data are presented graphically. The analysis is restricted to genes altered more than 1.5-fold in both groups. The fold-change in expression in the untreated antioxidant knockout mice (filled diamonds for *Sod1*$^{-/-}$, graphs **A** and **C**; open diamonds for *Gpx1*$^{-/-}$, graphs **B** and **D**) is on the y-axis, and that of WT mice treated with diquat is on the x-axis. Data for the 3 h time point are in graphs **A** and **B**, and data for the 6 h time point are in graphs **C** and **D**. Each symbol represents one specific gene whose x, y coordinates are given by its fold-level expression in antioxidant knockout mice (y) and WT mice treated with diquat (x), in both cases as compared to untreated WT-control mice. A least-square regression line was calculated for each data set, with the slope and R-square values indicated in each graph. There is a statistically significant correlation (P<0.001) for the diquat *vs. Sod1*$^{-/-}$ comparison but not for the diquat *vs. Gpx1*$^{-/-}$ comparison (especially note the large number of data points in the lower right quadrant of graph B and D, i.e., genes altered in opposite directions in both groups).

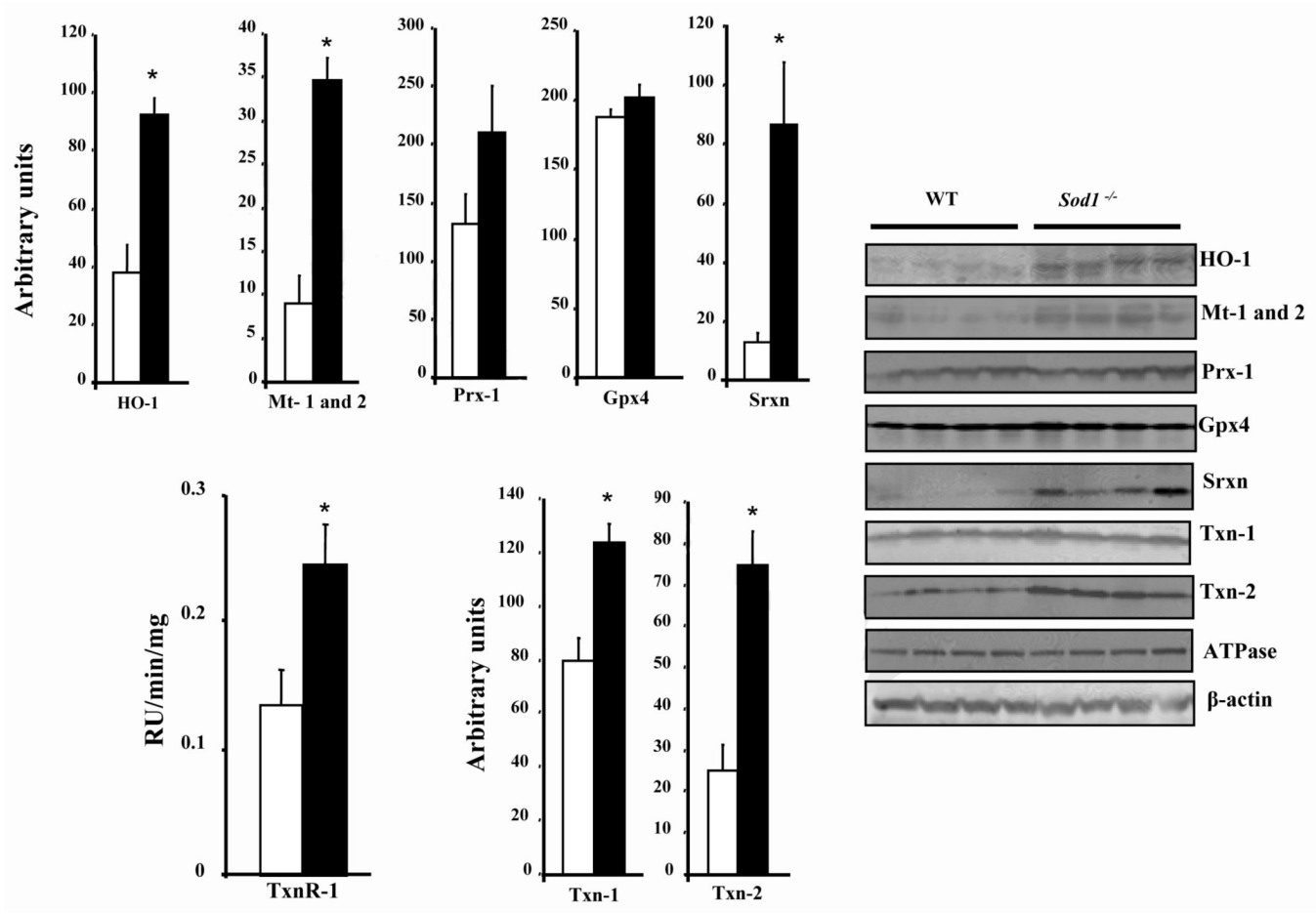

Figure 5. Antioxidant proteins upregulated in Sod1$^{-/-}$ mice

Proteins levels of selected antioxidant genes were measured by Western blots and enzymatic activity (thioredoxin reductase) in *Sod1*$^{-/-}$ (close bars) and WT mice (open bars). Hemeoxygenase 1 (HO-1), metallothionein (Mt) 1 and 2 (the proteins are too similar to be distinguished by size or antigenicity), thioredoxin-1 (Txn1), peroxiredoxin 1 (Prx-1), glutathione peroxidase 4 (Gpx4), sulfiredoxin (Srxn1), and thioredoxin reductase activity (TxnR) were measured in the cytosolic fraction of the liver. Thioredoxin-2 (Txn2) was measured in the mitochondrial fraction of the liver. The results are the mean of 4-5 animals ± SEM, and the asterisks denote those values significantly different from WT mice at the $p<0.05$ level.

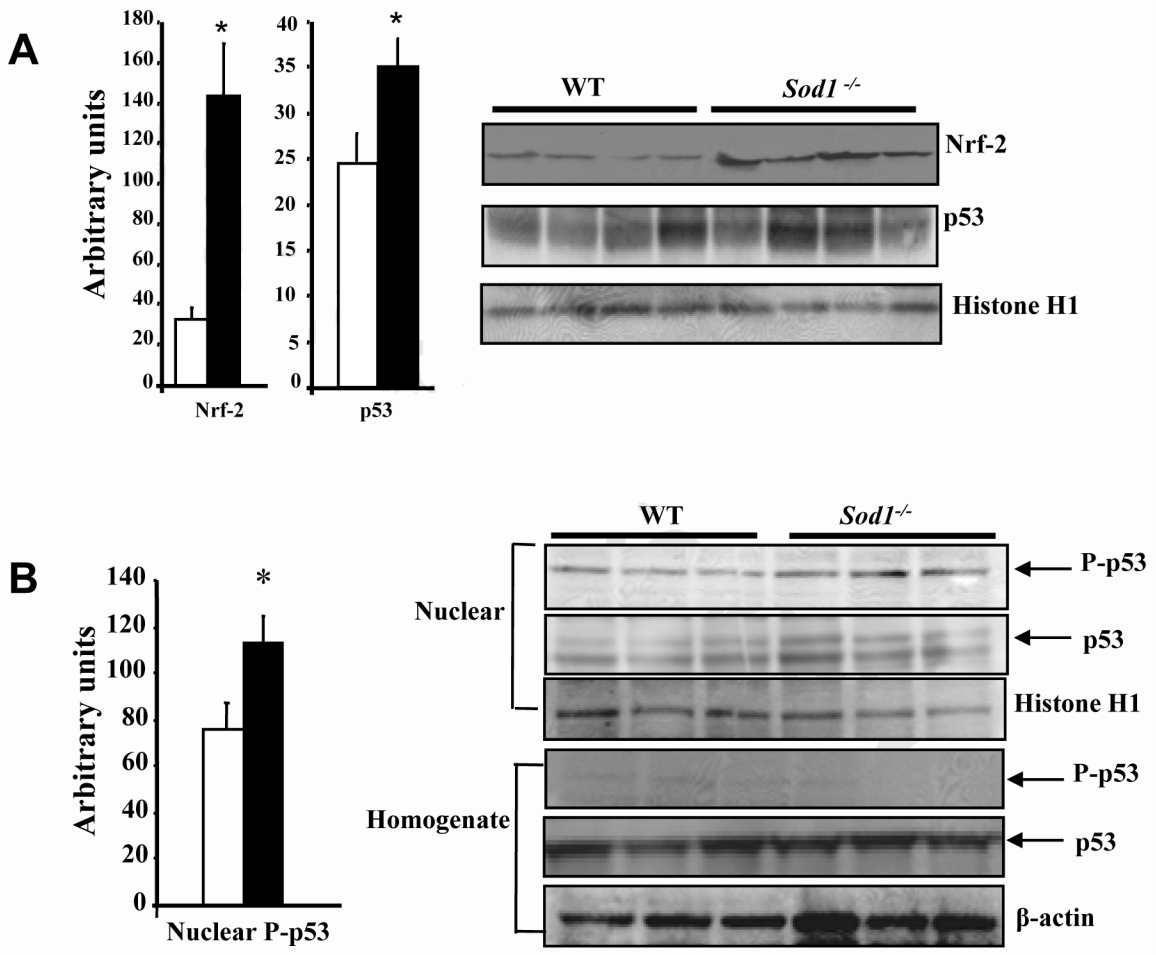

Figure 6. Increased nuclear levels of p53 and Nrf2 in Sod1$^{-/-}$ mice

The nuclear fraction from the livers of *Sod1*$^{-/-}$ (closed bars) and WT (open bars) mice were analyzed by Western blots as we described in the Experimental Procedures and expressed as a arbitrary units relative to the loading control, histone H1. **Graph A:** Total Protein levels of *p53* and *Nrf2* in nuclear extracts. **Graph B:** Phospho-p53 levels in nuclear and total homogenate extracts. The data are the mean of 3-4 animals ± SEM, and the asterisks denote those values significantly different from WT mice at the $p<0.05$ level.

TABLE I

Similarities between expression patterns of diquat-treated WT mice and Gpx1$^{-/-}$ or Sod1$^{-/-}$ untreated mice

The total number of genes meeting the indicated fold changes is noted in parenthesis. The number of genes showing common alterations between WT treated mice and untreated *Sod1*$^{-/-}$ or *Gpx1*$^{-/-}$ mice, is indicated below. For example, of the 81 genes upregulated by diquat more than 2.5-fold (Column 4), 13 were also upregulated more than 1.5-fold in the untreated *Sod1*$^{-/-}$ mice (Row 4).

Number of genes upregulated (compared to untreated WT)	**Diquat (3 or 6 h) (Fold Changes)**			
	All (896)	**>↑1.5 (321)**	**>↑2.0 (130)**	**>↑2.5 (81)**
	(Alterations in Common)			
↑*Gpx1*$^{-/-}$ (245)	20	6	2	1
↑*Sod1*$^{-/-}$ (638)	70	31	21	14
>↑1.5 *Gpx1*$^{-/-}$ (29)	5	2	2	1
>↑1.5 *Sod1*$^{-/-}$ (135)	35	26	18	13
Number of genes downregulated	All (1054)	>↑31.5 (235)	>↑2.0 (52)	>↑2.5 (14)
↑Gpx1$^{-/-}$ (403)	43	8	2	4
↓Sod1$^{-/-}$ (766)	51	15	5	0
>ș1.5 Gpx1-$^{-/-}$ (80)	7	4	2	1
>ș1.5 Sod1$^{-/-}$ (163)	15	11	5	0

TABLE II

Genes altered by both exogenous and endogenous oxidative stress

A list of genes showing a significant difference of greater than 1.5-fold when we compared untreated WT mice with either WT mice treated with diquat or untreated *Gpx1*$^{-/-}$ and *Sod1*$^{-/-}$ mice. Duplicates (by gene name or unigene ID) were removed.

Gene Symbol	Gene Name	1h DQ	3h DQ	6h DQ	12h DQ	*Gpx1*$^{-/-}$	*Sod1*$^{-/-}$
Igfbp1	insulin-like growth factor binding protein 1	6.42	7.72	6.96	6.22		5.23
Mt1[b]	metallothionein 1	2.88	5.87	7.52	8.29		4.52
Atf3[abc]	activating transcription factor 3		2.10				3.40
Pdk4[b]	pyruvate dehydrogenase kinase, isoenzyme 4		5.27	4.10	12.53		3.27
Apoa4	apolipoprotein A-IV			2.62	13.67		3.26
Tubb2	Tubulin, beta 2	1.85	2.07	2.45	3.50	*2.76*	2.68
Copeb[b]	Kruppel-like factor 6 (Klf6)		2.02	2.04	1.57		2.58
Rsb30	RAB30, member RAS oncogene family		7.64	7.31	18.57		2.50
3110043O21Rik	RIKEN cDNA 3110043O21 gene	2.10	3.27	2.30	3.74		2.41
Mtap	methylthioadenosine phosphorylase		2.87	3.87	4.66		2.27
Ddit4[abc]	DNA-damage-inducible transcript 4	5.04	5.65	8.43	6.20		2.27
Orm2	orosomucoid 2			2.04	3.80		2.20
Cdkn1a[abc]	cyclin-dependent kinase inhibitor 1A (P21)		4.27	8.52	14.50		2.12
Hist 1h1c	Histone 1, H1c			1.75	2.76		2.08
St5	suppression of tumorigenicity 5			1.89	4.24		2.05
Gdf15[ac]	Growth differentiation factor 15	2.26	3.72	1.98			1.91
Ndrg1[ab]	N-myc downstream regulated gene 1			1.82			1.89
Trp53inp1[a]	transformation related protein 53 inducible nuclear protein 1	1.94	2.67	2.29	1.77		1.83
Arl4	ADP-ribosylation factor-like 4	1.47	1.67	1.44	2.31		1.81
Enc1	ectodermal-neural cortex 1		1.56		2.32		1.66
5730438N18Rik	RIKEN cDNA 5730438N18 gene		2.14	2.29	1.69		1.61
Ifrd1	interferon-related developmental regulator 1	1.55	3.66	2.62	2.45		1.58
Ube2g2	ubiquitin-conjugating enzyme E2G 2		1.38	1.80	1.76		1.52
Stard4	StAR-related lipid transfer (START) domain containing 4	−1.45	−1.62	−1.90	−4.95		−1.69
3100002L24Rik	RIKEN cDNA 3100002L24 gene	−1.53	−2.07	−2.32	−2.57		−1.54
Gpr146	G protein-coupled receptor 146	−1.48	−1.32	−1.50	−1.68	*−1.72*	−1.68
D5Ertd593e	DNA segment, Chr 5, ERATO Doi 593, expressed		−1.37	−1.91	−3.67		−1.81
Fzd8	frizzled homolog 8 (Drosophila)	−1.40		−1.52	−1.38		−1.63
Aacs	acetoacetyl-CoA synthetase	−1.71	−1.96	−1.93	−1.88		−2.12
2210418O10Rik	RIKEN cDNA 2210418O10 gene		−1.46	−1.63	−2.10		−1.83

Gene Symbol	Gene Name	1h DQ	3h DQ	6h DQ	12h DQ	*Gpx1*$^{-/-}$	*Sod1*$^{-/-}$
4933439C20Rik	RIKEN cDNA 2210418O10 gene		−1.74	−2.17	−3.19		−1.59
Pcmtd2	protein-L-isoaspartate (D-aspartate) Omethyltransferase domain containing 2		−1.82	−2.23	−4.52	*−1.69*	−1.76
Pcmtd2	protein-L-isoaspartate (D-aspartate) Omethyltransferase domain containing 2		−1.82	−2.23	−4.52	−1.69	−1.76
Lect1	leukocyte cell derived chemotaxin 1	−1.30	−1.52	−2.14	−2.64		−2.57
Hsd3b5	hydroxysteroid dehydrogenase-5, delta<5>-3-beta			−2.27	−9.84		−5.82

*a*indicates that the gene is a p53 target based on references (44,46);

*b*indicates that the gene is altered in the same direction by paraquat in heart previously described by Edwards et al. (21);

*b*indicates that the genes are altered in the same direction in human MCF7 and MRC9 cells in response to 100μM H2O2 as described by Desaint et al. (19).

TABLE III

Genes hyper-inducible or hyper-repressible by diquat in antioxidant knockout mice

A list of genes showing the greatest difference when we compared diquat-treated WT mice with diquat-treated knockout mice (either *Sod1*$^{-/-}$ or *Gpx1*$^{-/-}$). Duplicates (by gene name or unigene ID) were removed. In columns 1 to 10; the fold expression is expressed with reference to untreated WT control mice, while in columns 11 and 12, the data are expressed with respect to WT mice 1 h after diquat injection.

Gene Symbol	Gene Name	1h DQ	3h DQ	6h DQ	12h DQ	Gpx1$^{-/-}$	Sod1$^{-/-}$	Gpx1$^{-/-}$ 1h DQ	Sod1$^{-/-}$ 1h DQ	Gpx1$^{-/-}$ 1h DQ vs WT 1h DQ	Sod1$^{-/-}$ 1h DQ vs WT 1h DQ
Atf3[abc]	activating transcription factor 3		2.10				3.40	2.29	13.76	1.95	11.70
Copeb[b]	Kruppel-like factor 6 (Klf6)		2.02	2.04	1.57		2.58	1.93	4.90	1.86	4.72
Tiparp	TCDD-inducible poly(ADPribose) polymerase		4.06	4.21	3.59			3.60	3.86	3.09	3.31
H3f3b	H3 histone, family 3B		2.34	2.96	3.22		1.23	1.74	2.25	1.56	2.02
Rgs16	regulator of G-protein signaling 16			2.93		*−1.71*		2.57		3.07	
1200016E24Rik	RIKEN cDNA 1200016E24 gene		3.43	3.40	4.33			1.95	2.90	1.36	2.01
Jun	Jun oncogene	1.81	3.01	2.30	2.78			4.23	9.40		5.20
Btg2[abc]	B-cell translocation gene 2, ant iproliferative	2.52	3.55	2.61	3.82			4.60	12.45		4.95
Plk3[a]	Polo-like kinase 3 (Drosophila)		3.17	1.85	2.28			2.34	3.34		2.47
Ifrd1	interferon-related developmental regulator 1	1.55	3.66	2.62	2.45		1.58	2.82	3.30		2.13
Apoa4	Apolipoprotein A-IV			2.62	13.67		3.26		5.48		5.29
Orm2	Orosomucoid 2			2.04	3.80		2.20		5.11		4.73
Ets2	E26 avian leukemia oncogene 2, 3' domain		1.84	2.09	2.51		1.37		2.20		2.38
Klf4	Kruppel-like factor 4 (gut)		2.36	1.88	2.19			2.74	2.20		2.27
Gdf15[ac]	growth differentiation factor 15	2.26	3.72	1.98			1.91		4.97		2.20
Itsn1	Intersectin 1 (SH3 domain protein 1A)			−2.27	−3.39					−2.70	
Lect1	leukocyte cell derived chemotaxin 1		−1.52	−2.14	−2.64		−2.57		−3.00		−2.31
Keg1	Kidney expressed gene 1			−2.11	−7.47				−2.61		−2.61
Hsd3b5	hydroxysteroid dehydrogenase-5, delta<5>-3-beta			−2.27	−9.84		−5.82	−19.97	−24.65	−18.75	−23.14

[a] indicates that the gene is a p53 target based on references (44,46))

[b] indicates that the gene is altered in the same direction by paraquat in heart as described by Edwards et al. (21);

[c] indicates that the genes is altered in the same direction in human MCF7 and MRC9 cells in response to 100μM H2O2 as described by Desaint et al. (19).

TABLE IV

Genes with antioxidant function upregulated in the Sod1$^{-/-}$ mice

A list of antioxidant or allied function genes significantly upregulated in the *Sod1*$^{-/-}$ mice compared to untreated WT mice or *Gpx1*$^{-/-}$ mice.

AffyMetrix Probeset ID	Gene Symbol	Gene Name	Fold Change	Adjusted p-value
1422557_s_at	Mt1^{M*}	metallothionein 1	4.52	0.0036
1427473_at	Gstm3^{N}	Glutathione S-transferase, mu 3	3.20	0.0000
1451260_at	Aldh1b1	aldehyde dehydrogenase 1 family, member B1	2.85	0.0005
1425351_at	Srxn1N	Sulfiredoxin 1 homolog (S. cerevisiae)	2.29	0.0000
1416101_a_at	Hist1h1c	histone 1, H1c	2.08	0.0001
1424296_at	Gclc^{N}	glutamate-cysteine ligase, catalytic subunit	1.96	0.0000
1421041_s_at	Gsta1^{N}	Glutathione S-transferase, alpha 1 (Ya)	1.64	0.0017
1455640_a_at	Txn2^{N}	thioredoxin 2	1.51	0.0009
1460561_x_at	Sepw1^{M}	Selenoprotein W, muscle 1	1.45	0.0001
1424433_at	Msrb2	Methionine sulfoxide reductase B2	1.41	0.0003
1424487_x_at	Txnrd1^{N*}	thioredoxin reductase 1	1.27	0.0042
1456193_x_at	Gpx4	Glutathione peroxidase 4	1.19	0.0032
1416000_a_at	Prdx1^{N}	Peroxiredoxin 1	1.18	0.0021
1460167_at	Aldh7a1	aldehyde dehydrogenase family 7, member A1	1.16	0.0004
1452823_at	Gstk1^{N}	Glutathione S-transferase kappa 1	1.14	1.14

*indicates genes previously shown to be induced in Sod1−/− mice (26,51).

^{M}known target of Nrf2 (48)

^{N}known target of Mtf1 (86)